Chapter 3

Musa champa (Chinichampa) peduncle derived catalyst for biodiesel synthesis

3.1 Introduction

The encouragement of searching for new plant based heterogeneous catalyst for biodiesel synthesis is attracting researchers from the last few decades. A number of *Musa* species have been reported as the catalyst sources for the preparation of biodiesel such as *Musa balbisiana* Colla [11,111], *Musa acuminata* peel [108,136], *Musa paradisiaca* peel, trunk and rhizome [169], banana peel [105], etc., whereas peduncle of *Musa species* is less commonly being reported as catalyst in biodiesel synthesis. In this chapter, based on the idea of highly basic nature of the plant-based ash material, an efficient heterogeneous catalyst was prepared from waste *Musa champa* peduncle and employed in the synthesis of biodiesel from *Jatropha curcas* oil.

Banana and plantains are horticultural crops belonging to the family of Musaceae, the second-largest produced fruit, cultivated in nearly 130 countries in the humid and subhumid tropical regions and are considered the 4^{th} most important global food-crop [235,236]. It is possibly the oldest cultivated crop with high nutritional value, with an approximate production of 106 million tons yearly, meeting world demand for about 16 % of the total food production [237]. Bananas are an important part of the diet as an affluent source of carbohydrates, having a calorific value of 67 calories per 100 g [238]. Due to existence of high-fiber content, bananas are capable of lowering cholesterol, relieving constipation and preventing colon cancer, as well as their high potassium content helps in the prevention of high blood pressure and muscle cramps [235,239]. Banana is also a part of traditional medicine due to its therapeutic value and is used in the treatment of uremia, dysentery, diarrhea, intestinal lesion in ulcerative colitis, diabetes, cardiac disease, nephritis, etc. [240]. Worldwide production of bananas generates huge post-harvest wastes such as trunk or stem, peel, rhizome and peduncle, which are also being reported in the preparation of various value-added products. The largest waste part of the banana plant is the stem, which is successfully utilized in the extraction of fiber with good tensile strength in comparison to other natural fibers such as coir, jute, palm, etc. for industrial usage [239,241]. The literature revealed the utilization of waste banana trunk (stem) for the

extraction of fiber for application in textile industries as well as in the preparation of yarn, fabric, etc. [238,242]. The waste banana plant is extensively used in the making of paper, packing materials, ropes, etc., with virtuous results [243,244]. In recent times, biochar prepared from the banana plant is utilized in the removal of toxic substances and dye degradation from wastewater [245,246]. Banana fruit peel waste with good carbohydrate and mineral contents is also reported to be used for the production of sugar [247]. Waste peduncle of banana plant with enriched K content was reported for the preparation of biochar for K supplement in soil [248]. In the field of catalysis for biodiesel synthesis, preparation of biocatalyst from the peel, trunk and rhizome of a variety of bananas were reported with notable results [11,105,111,169]. However, the banana peduncle with high K content is least utilized as heterogeneous catalyst for the preparation of value-added products, which may execute good efficiency in biodiesel synthesis.

Musa champa banana commonly known as Chinichampa in Assam belonging to the family of Musaceae possesses AB Genome of Ney Poovan subgroup and is widely cultivated in the foothill of Himalaya in the Northeast region of India, Bangladesh as well as other parts of the world [249,250]. Due to its exceptional sweet and sub-acid taste and attractive fresh banana aroma, it is popular among banana lovers. *M. champa* grown in rain-fed conditions with minimal irrigation procedure produces a small and thin peel containing nearly 150-250 fingers. Due to the huge cultivation of *M. champa*, the enormous waste peduncle is generated with management issues to the environment. Thus, waste *M. champa* peduncle has a high potential for the development of value-added materials. One potential area is the preparation of solid material from *M. champa* peduncle and effective utilization of it as the catalyst for biodiesel synthesis, which has not yet been reported in the literature. This study investigates the preparation, characterization and catalytic property evaluation of heterogeneous base catalyst from waste *M. champa* peduncle in biodiesel synthesis. Here, the burnt ash and calcined materials were employed as catalysts for the transformation of *Jatropha curcas* oil to biodiesel along with the kinetics and thermodynamic studies. The effects of catalyst load, temperature of the reaction, methanol to oil ratio (MTOR) and catalyst leaching and recyclability were also studied and reported along with the composition of the prepared catalysts.

3.2 Materials and methods

3.2.1 Materials

Post-harvest *Musa champa* peduncle is collected from Debargaon village of Assam's Kokrajhar district, India for the catalyst preparation. Non-edible (*Jatropha curcas*) oil obtained

from Harvi Trading Company, Udaipur, Rajasthan, India was utilized for transesterification to explore the efficiency of the catalyst. The chemicals used in this study are mentioned in **Chapter 2** (**Section 2.2.1**, **Page no. 27**).

3.2.2 Methods

3.2.2.1 Preparation of catalyst

The collected post-harvest waste *M. champa* peduncle was sliced into small portions (**Fig. 3.1**) and dried under the sun for about 15 days. The dried materials of peduncle were then completely burnt in the open air to ash. The calcination of ash materials was carried out using a programable furnace at 550 ^{o}C for 2 h, kept in a desiccator and crushed to a fine powder with the help of a mortar and pestle. The finely powdered ash and the calcined ash materials were characterized and investigated as a catalyst in transesterification of jatropha oil to biodiesel.

Fig. 3.1. *M. champa* peduncle (B) obtained from harvesting fruit (A), cut into pieces (C), sun dried (D), burnt ash (E) and calcined catalyst (F).

3.2.2.2 Catalyst characterization

The XRD spectrum was recorded from an X-ray diffractometer (ULTIMA IV, Rigaku, Japan) for the investigation of the qualitative composition of the *M. champa* peduncle catalyst. FT-IR, BET and XPS analyses were carried out as mentioned in **Chapter 2** (**Section 2.2.2.2**, **Page no. 28–29**). The catalyst was studied for the structural information using HR-TEM images and SAED pattern which was recorded using the TEM instrument (Thermo Fischer,

Talos F200 S). The pH value was determined as per the method mentioned in **Chapter 2** (**Section 2.2.2.2**, **Page no. 29**). The basicity and turnover frequency (TOF) were determined following the procedure mentioned in **Chapter 2** (**Section 2.3.1.8**, **Page no. 46–47**).

3.2.2.3 Biodiesel synthesis and characterization

The synthesis of biodiesel was performed using *M. champa* peduncle burnt ash catalyst and its calcined catalyst as per the procedure mentioned in **Chapter 2** (**Section 2.2.2.3**, **Page no. 29**). Characterizations of oil and biodiesel by FT-IR and NMR were done as mentioned in **Chapter 2** (**Section 2.2.2.3**, **Page no. 30**). The compositions of methyl esters of the biodiesel were examined using a Gas Chromatography-Mass Spectrophotometer (Perkin Elmer, Claurus 680 GC, 60.0 m × 250 μm column, 600C MS). The operational procedure includes keeping the temperature initially at 60 ^{o}C for 6 min followed by increasing it to 180 ^{o}C at the rate of 5 ^{o}C per min, then further increasing it to 280 ^{o}C at the rate of 10 ^{o}C per min. The sample was injected by dropping the temperature to 250 ^{o}C after 20 min. The carrier gas used was He, the mass scan was from 50-500 Da and the transfer and source temperature were respectively 180 ^{o}C and 160 ^{o}C. The properties of produced jatropha biodiesel were also determined according to the procedure mentioned in **Chapter 2** (**Section 2.2.2.3**, **Page no. 30**).

3.3 Results and discussion

3.3.1 Characterization *Musa champa* peduncle catalyst

3.3.1.1 Powder XRD analysis

Fig. 3.2 showed the powder XRD pattern of *M. champa* peduncle catalyst calcined at 550 ^{o}C. The crystalline components in the catalyst were investigated by comparing the 2θ data with that of JCPDS (ICDD 2003) as well as by referring to the reported literature. This study revealed the occurrence of a mixture of components such as K_2CO_3, K_2O, KCl, CaO, $CaCO_3$, $MgCO_3$, MgO, Fe_2O_3, Na_2CO_3, SiO_2, SrO_3, ZnO and $CaMg(CO_3)_2$. The XRD 2θ values at 28.54, 40.75, 49.78 and 58.62 represented the KCl present in the catalyst. Similar 2θ values for KCl in the Malbhog peel, trunk and rhizome catalysts were also reported [169]. The existence of K_2CO_3 in the catalyst was represented with the 2θ values at 26.85, 29.80, 31.10, 31.92 and 41.49. The high intense peak at the 2θ value of 31.92 may be due to the high K content in the catalyst in the form of K_2O or K_2CO_3. K_2O was also found to be present and was characterized from the 2θ values of 25.95, 27.51, 32.56, 39.37, 46.73, 48.38, 51.42, 51.70 and 56.93 [205,206,234]. The 2θ values at 32.31, 37.06, 37.43, 66.55, 67.48 and 67.81 indicated CaO in

the catalyst, whereas the 2θ value at 36.90 showed the presence of $CaCO_3$. Magnesium in the form of MgO (2θ = 43.18, 43.65) and $MgCO_3$ (2θ = 34.09) was also found to be present (**Fig. 3.2)**. The occurrence of Fe_2O_3 in the catalyst was revealed from the 2θ values of 24.06 and 32.87. The 2θ value at 37.96 indicated the presence of Na_2CO_3. The silicon in the form of SiO_2 was exposed by the XRD pattern at 2θ 21.60 and 28.07. The peaks at 2θ values of 51.0 and 45.54 indicated the presence of SrO and $CaMg(CO_3)_2$ in the catalyst. Zn in the form of ZnO was represented by the 2θ values at 36.41, 47.6 and 62.9 in the XRD spectrum of catalyst. This analysis depicted the occurrence of oxides and carbonates of various metals along with KCl demonstrating that K is a dominating element in the catalyst.

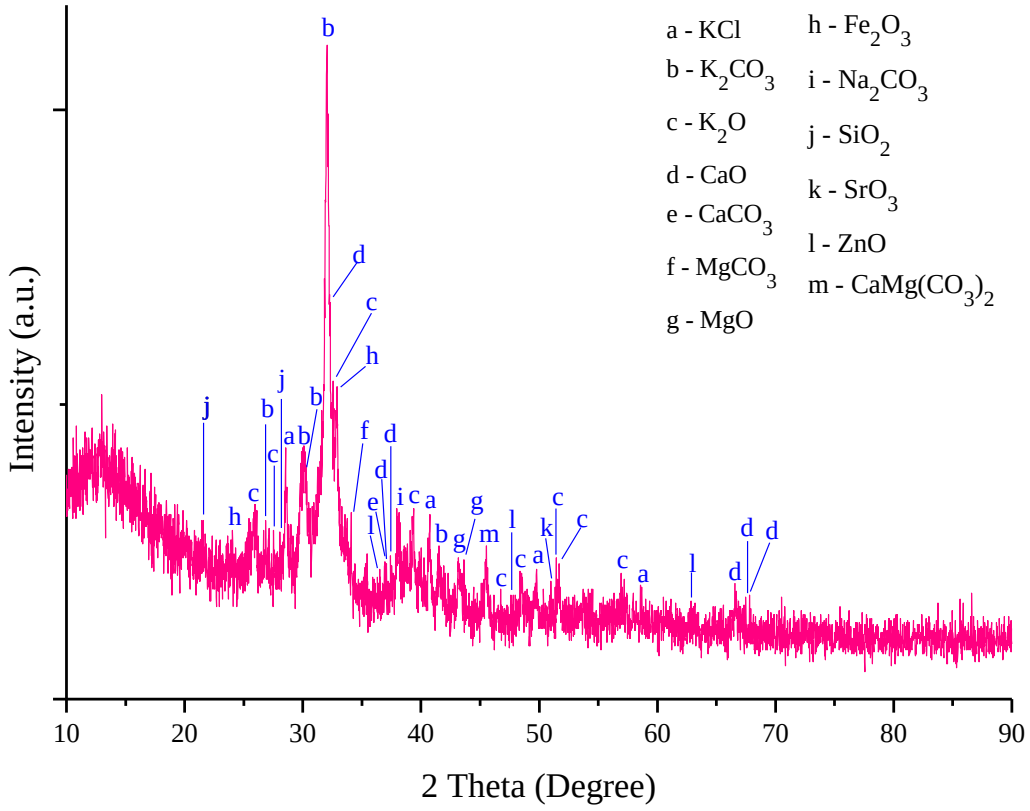

Fig. 3.2. XRD pattern of *M. champa* peduncle catalyst calcined at 550 °C.

3.3.1.2 FT-IR analysis

The FT-IR patterns of the catalyst calcined 550 °C (A) and burnt ash (B) catalyst are depicted in **Fig. 3.3**. The adsorption of H_2O on the surface of *M. champa* peduncle catalyst was indicated by the broad absorption peak at 3494 cm^{-1} in both the catalysts [94,251]. A similar absorption peak at 3434 cm^{-1} was reported by Fadhil et al. [252] for the hydroxyl group attached to the catalyst particle. The absorption band at 2400 to 2000 cm^{-1} depicts the stretching

vibration of M-O-K and accordingly, the peak at 2177 cm^{-1} observed in the spectrum of burnt ash catalyst may be due to M-O-K (M = Si, Mg, etc.) stretching vibrations [108,109]. However, calcination of the catalyst at 550 ^oC, the peak for the M-O-K bond was not observed which may be due to the dissociation of M-O from the M-O-K bond resulting in the formation of oxide and carbonates of metals. The presence of metal carbonates like K_2CO_3 and $CaCO_3$ in the catalysts was attributed to the absorption due to C-O stretching frequency at 1647, 1399 and 1129 cm^{-1} in burnt ash and 1641, 1399 and 1123 cm^{-1} in the calcined catalyst. This conforms with XRD spectrum (**Fig. 3.2**) which also supported the existence of metal carbonates in the calcined catalyst. This study agrees with the findings reported by Gohain et al. [220], Betiku et al. [115] and Etim et al. [107]. The presence of the Si-O-Si bond in the catalysts was signified by the peaks at 1042 and 864 cm^{-1} in burnt ash and 1020 and 870 cm^{-1} in the calcined catalyst and agrees with the XRD analysis (**Fig. 3.2**). The absorption peaks at 703, 647 and 619 cm^{-1} in burnt ash and 697 and 622 cm^{-1} in calcined catalyst were observed due to Ca-O and K-O bond vibration demonstrating the presence of K_2O and CaO in the catalysts. In accordance with the XRD analysis, the FT-IR results also showed the occurrence of carbonates and oxides of metals in both the catalysts.

3.3.1.3 Determination of surface area, pore size and pore volume

BET surface area analysis of the *M. champa* peduncle catalyst calcined at 550 ^oC resulted in a surface area of 8.57 $m^2\ g^{-1}$. Gohain et al. [109] reported a similar surface area for catalyst generated from *Musa balbisiana* peel. However, Basumatary et al. [169] reported a comparably lower surface area for the catalyst prepared from Malbhog peel (4.119 $m^2\ g^{-1}$), Malbhog trunk (6.418 $m^2\ g^{-1}$) and Malbhog rhizome (7.019 $m^2\ g^{-1}$) with proficient catalytic activity in transesterification. Lower surface areas were reported in the catalyst of *M. balbisiana* trunk (1.487 $m^2\ g^{-1}$) [11], Tucumã peel (1.0 $m^2\ g^{-1}$) [12], *M. acuminata* peel (1.4546 $m^2\ g^{-1}$) [108] and gasified straw slag (1.266 $m^2\ g^{-1}$) [223] with considerable catalytic activity. A higher surface area of 39.0 and 38.710 $m^2\ g^{-1}$ for ash catalyst obtained from *M. balbisiana* underground stem was reported by Sarma et al. [111] and Aslam et al. [110]. The N_2 adsorption-desorption (**Fig. 3.4**) of the catalyst was found to be matching with type IV isotherm along with the H3 hysteresis loop which conforms with the BDDT (Brunauer-Deming-Deming-Teller) classification [220]. This revealed the mesoporous structure of the catalyst with little extension to the microporous structure [104,169]. The BJH average pore volume and diameter of this catalyst was found to be 0.034 $cm^3\ g^{-1}$ and 3.71 nm. The pore size distribution of the catalyst was found to be from 1.928 nm to 6.376 nm (**Fig. 3.4**), which depicted the borderline micro-

mesoporous structure of material. A similar adsorption-desorption isotherm was also reported for the catalysts generated from Malbhog peel, trunk and rhizome [169] which indicated a micro-mesoporous structure.

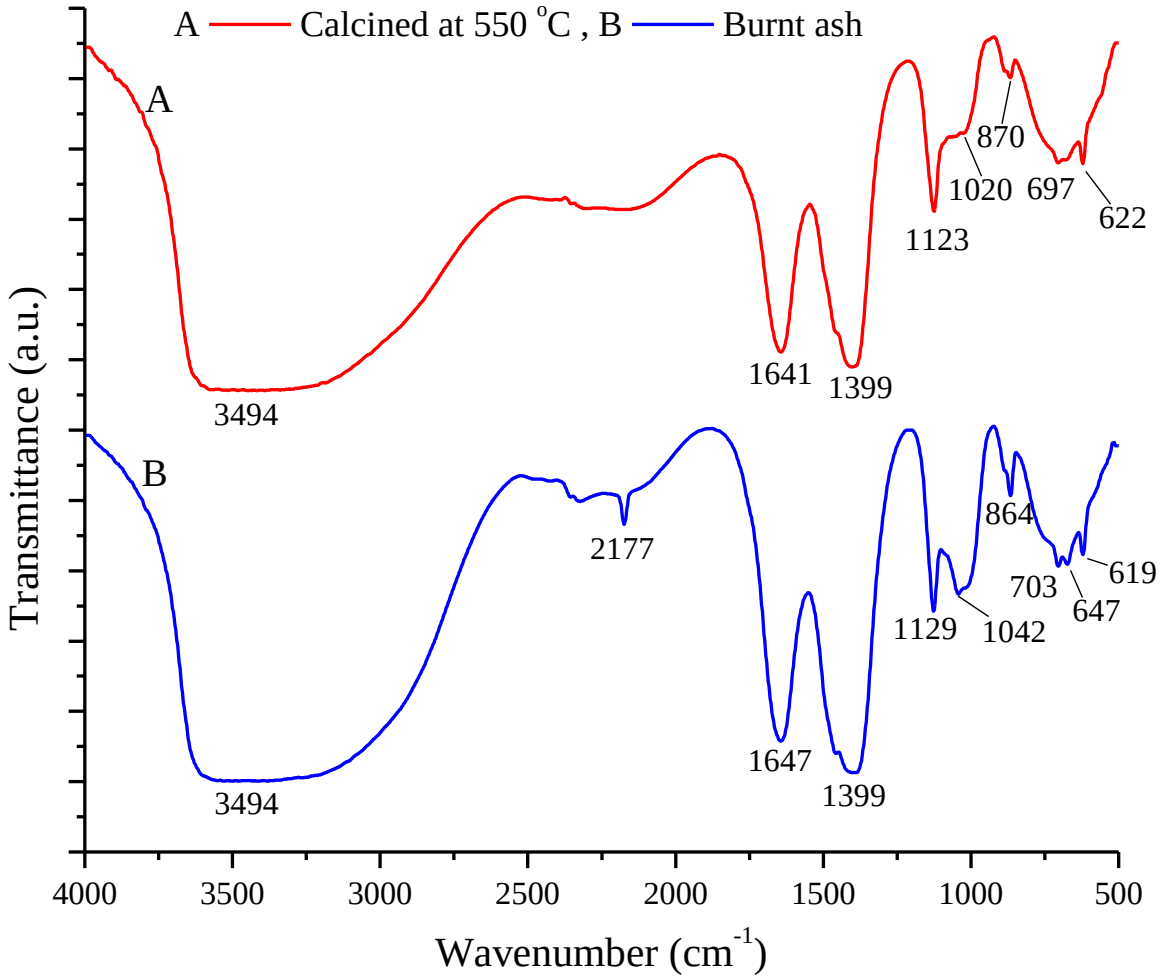

Fig. 3.3. FT-IR spectra of *M. champa* catalyst calcined at 550 °C (A) and burnt ash (B).

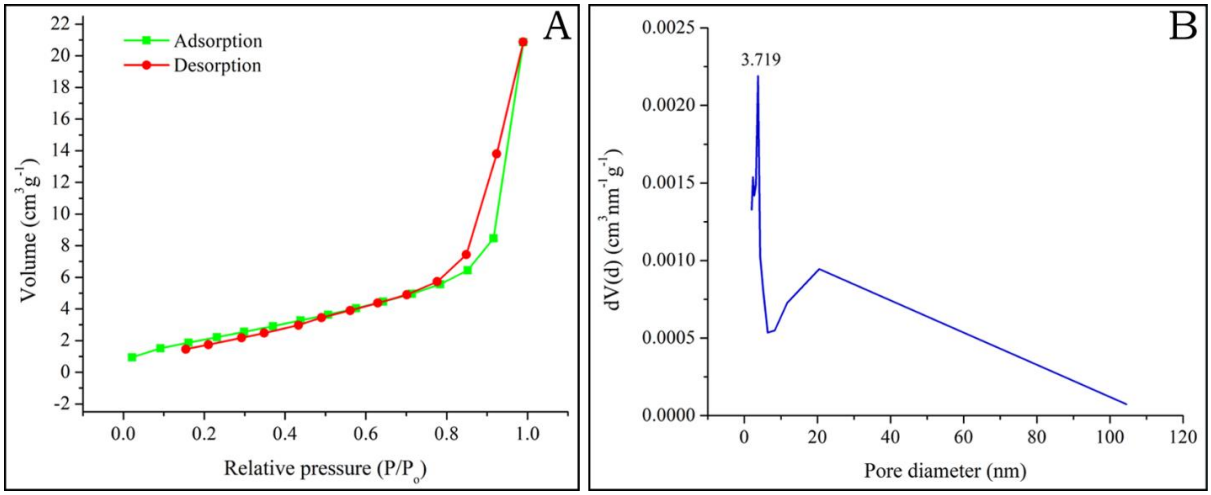

Fig. 3.4. N_2 adsorption-desorption isotherm (A) and adsorption pore size distribution (B) of *M. champa* peduncle catalyst calcined at 550 ^oC.

3.3.1.4 FESEM analysis

The surface morphologies of *M. champa* peduncle burnt ash, calcined and the 3rd reused catalysts are depicted in **Fig. 3.5** (A, B, C). The images exhibited the differences in the morphology of the catalysts. The burnt ash catalyst (**Fig. 3.5** A) showed clusters of agglomerated particles. The bright particles in the image might be due to oxygenated components like carbonates and oxides [113,169]. The catalyst on calcination (550 ^oC, 2 h) showed slight changes and the agglomerated morphology remained intake (**Fig. 3.5** B). However, a complete change in the morphological structure of the 3rd recycled catalyst was observed (**Fig. 3.5** C), which depicted non-uniform sizes and shapes of sheet-like and layered type structures.

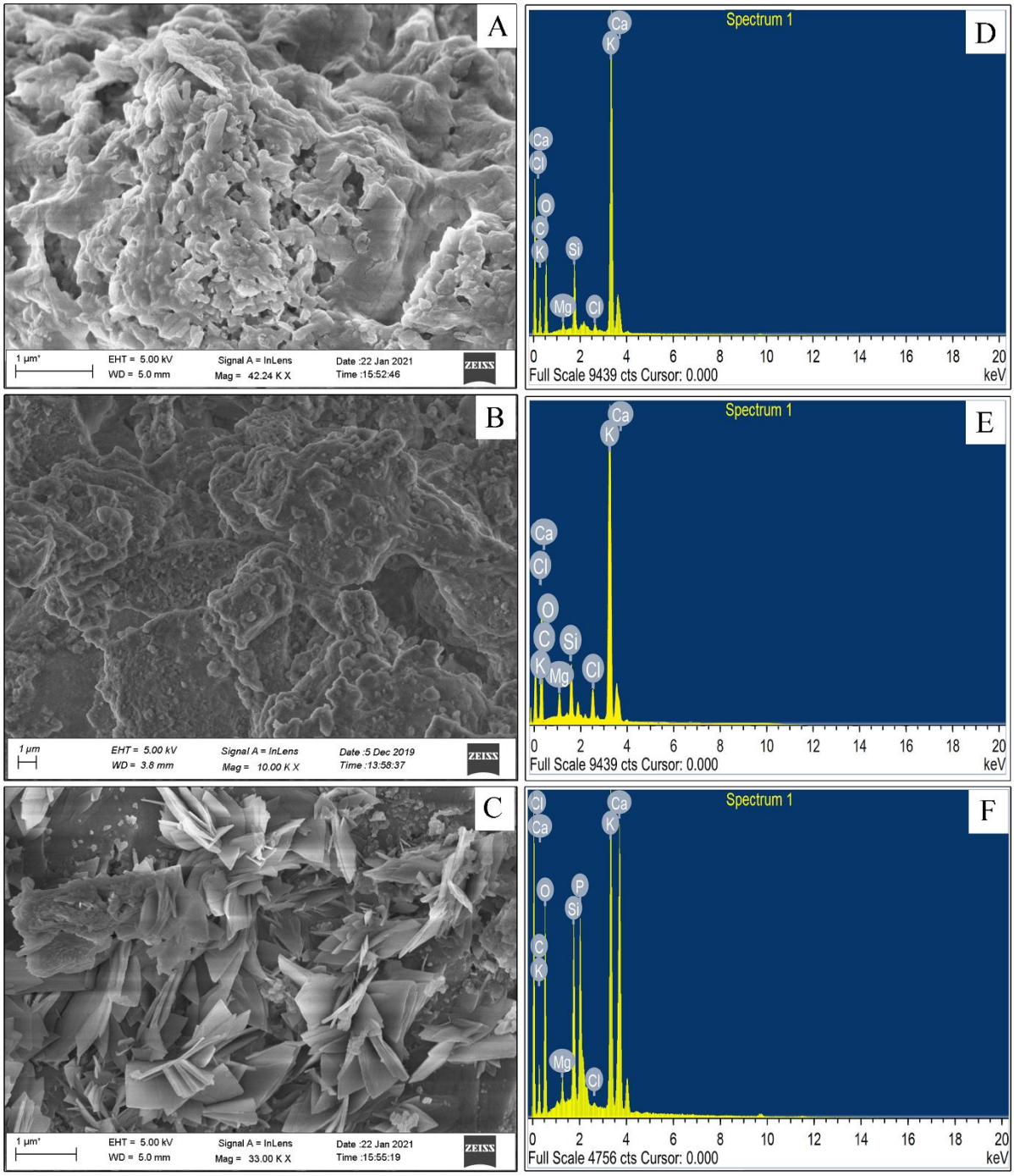

Fig. 3.5. SEM images (A, B, C) and EDX patterns (D, E, F) of *M. champa* peduncle burnt ash (A, D), catalyst calcined at 550 ^{o}C (B, E) and its 3rd recycled catalyst (C, F).

3.3.1.5 Elemental composition studies

EDX analyses {**Fig. 3.5** (D, E, F)} were executed to know the elemental composition of the peduncle catalysts and 3rd recycled catalyst and the results are summarized in **Table 3.1**. Remarkably, the amount of K was recorded to be the highest among the metals present. The K content in burnt ash catalyst, calcined catalyst and 3rd recycled catalyst was found to be 31.88,

51.93 and 13.20 wt. %, respectively. It is observed that K composition increased on calcination as compared to the burnt ash catalyst. The calcined catalyst on repeated use in transesterification up to the 3rd cycle, the K concentration decreased (**Table 3.1**) which may be due to leaching during the catalyst regeneration process. A significantly high amount of oxygen along with a moderate concentration of carbon was also noticed in the catalysts (**Table 3.1**) indicating the occurrence of carbonate and oxide of K in the form of K_2CO_3 and K_2O, which is supported by XRD (**Fig. 3.2**) and FT-IR (**Fig. 3.3**) patterns. It is revealed that the attribution of high efficacy of biomass ash catalyst is due to the high K content in the form of K_2O and K_2CO_3 [112,129]. Betiku et al. [115] stated that the presence of high K in the catalyst is ascribed to show prominent catalytic efficiency in the synthesis of biodiesel. Mendonça et al. [44] also specified that heterogeneous catalysts derived from waste-biomass with high alkali metal content possessed efficient activity in the transesterification of oil to biodiesel. A comparison of the composition of *M. champa* peduncle catalysts with other banana-based catalysts and other waste plant-based catalysts is listed in **Table 3.2**. It is to be noted that the catalysts prepared from *Carica papaya* stem (56.71 wt. %) [220], *M. paradisiacal* peel (54.73 wt. %) [112] and banana peduncle (70.06 wt. %) [253] showed significantly high K concentrations and found to be comparable with the present peduncle catalyst of this study. However, other catalysts showed lower K contents (**Table 3.2**) which may be the reason for the lower catalytic efficacy for transesterification in comparison to *M. champa* calcined catalyst of this study.

Table 3.1: FESEM-EDX analyses of *M. champa* peduncle catalysts

Elements	**Burnt ash catalyst**		**Catalyst calcined at 550 °C**		**3rd recycled catalyst of calcined catalyst (550 °C)**	
	Weight %	**Atomic %**	**Weight %**	**Atomic %**	**Weight %**	**Atomic %**
C	14.90	24.19	2.48	5.29	15.60	24.79
O	44.81	54.64	30.38	48.65	45.78	54.61
K	31.88	15.90	51.93	34.02	13.20	6.44
Ca	2.65	1.29	4.72	3.01	13.84	6.59
Mg	0.70	0.56	1.83	1.93	0.90	0.71
Si	4.36	3.03	3.60	3.29	4.79	3.25
P	-	-	1.53	1.26	5.72	3.53
Cl	0.71	0.39	3.52	2.54	0.16	0.09

Table 3.2: Elemental composition comparison of *Musa champa* peduncle catalyst with other reported agro-wastes ash catalysts

Ash catalyst	Calcination conditions	Composition (%)													References
		Na	K	Ca	Mg	Al	Si	P	Cl	Fe	Mn	Zn	Sr	C	O	
Musa champa peduncle	550 °C, 2h	–	51.93	4.72	1.83	–	3.60	1.53	3.52	–	–	–	–	2.48	30.38	This work
Musa champa peduncle	-	–	31.88	2.65	0.70	–	4.36	–	0.71	–	–	–	–	14.90	44.81	This work
Musa balbisiana underground stem	550 °C, 2 h	0.61	25.09	10.44	10.04	4.07	35.92	4.47	–	1.88	–	–	1.89	–	–	[111]
Musa paradisiacal peels	700 °C, 4 h	–	51.02	–	1.15	0.29	2.51	1.84	6.27	–	–	–	–	–	36.43	[107]
Musa balbisiana peels	700 °C, 4 h	10.41	41.37	36.08	12.02	–	–	–	–	–	–	–	–	–	–	[109]
Musa paradisiaca peel	550 °C, 2 h	–	29.25	4.01	1.08	–	3.81	1.06	3.01	–	–	–	–	24.02	33.34	[169]

Musa paradisiaca trunk	550 °C, 2 h	-	36.31	2.21	3.08	0.63	2.84	1.12	2.13	0.59	-	-	-	13.22	37.87	[169]
Musa paradisiaca rhizome	550 °C, 2 h	-	30.06	3.06	0.69	-	1.67	1.00	1.83	-	-	-	-	18.43	43.27	[169]
Red banana peduncle	700 °C, 4 h	–	42.23	1.70	1.39	–	1.54	1.91	–	–	–	–	–	–	50.54	[224]
Red banana peduncle	Uncalcined	–	25.63	–	0.97	–	0.56	0.78	–	–	–	–	–	–	72.06	[224]
Banana peduncle	700 °C, 4 h	–	52.04	5.27	5.71	–	–	–	–	–	–	–	–	–	36.99	[253]
Lemna perpusilla Torrey	550 °C, 2 h	0.53	11.32	–	–	–	82.51	–	1.10	–	–	–	–	5.10	–	[114]
Acacia nilotica tree stem	500 °C	0.6	6.7	13.3	2.7	8.3	15.7	0.80	–	–	–	–	–	–	–	[136]
Carica papaya stem	700 °C, 4 h	14.78	56.71	21.08	4.41	–	3.02	–	–	–	–	–	–	–	–	[220]

Acacia nilotica tree stem	800 °C	5.7	5.7	17.8	4.5	1.2	21.5	0.5	–	–	–	–	–	–	–	[136]
Camphor tree leaf	800 °C, 2 h	0.23	1.22	12.05	1.82	2.70	–	–	–	–	–	–	–	–	–	[159]

The XPS studies (**Fig. 3.6**) were also conducted to investigate the surface elemental composition of the *M. champa* peduncle catalysts and the 3rd recycled catalyst **(Table 3.3**). The analysis established the presence of C, O, Na, Mg, K, Ca, Si, Mn, Fe, Sr, Zn and Cl in the catalysts. In line with FESEM-EDX data, the XPS analysis also demonstrated high concentrations of K (18.78 %), carbon (50.63 %) and oxygen (23.01 %) in the calcined catalyst indicating the predominant presence of K_2O, K_2CO_3 and KCl, which are also supported by XRD pattern (**Fig. 3.2**) and FT-IR spectra (**Fig. 3.3**). The XPS spectra of O 1s (**Fig. 3.6** B) showed binding energy of 530.83 eV for burnt ash, 530.52 eV for calcined catalyst and 531.23 eV for 3rd recycled catalyst demonstrating the occurrence of oxygen of the metal oxides. In the deconvoluted XPS patterns of C 1s (**Fig. 3.6** C), two peaks at binding energies of 284.79 and 288.57 eV for burnt ash, 284.90 and 289.07 eV for calcined catalyst and 284.88 and 288.59 eV for the 3rd reused catalyst were observed and these are due the sp^2 hybridized carbon (C=O) of the metal carbonates present in the catalyst [108,169,234]. The XPS spectra of K 2p (**Fig. 3.6** D) depicted two peaks at 292.45 and 295.25 eV in burnt ash, 292.45 and 295.20 eV in calcined catalyst and 292.89 and 295.70 eV in the recycled catalyst. The peaks at the lower binding energies corresponded to K $2P_{3/2}$, whereas the peaks at the higher binding energies indicated K $2P_{1/2}$, representing the +1 oxidation state of K in K_2O and K_2CO_3 [104,234]. This analysis also signified the presence of K_2O and K_2CO_3 that was projected by XRD analysis (**Fig. 3.2**). It is to be noted that the binding energy of K in K_2O is lower compared to K_2CO_3 as the K–O bond in K_2O is less ionic with lower polarizability of K compared to that of K_2CO_3. This can be explained by the fact that the relative covalency of carbon in K_2CO_3 enhances the ionic character of K and subsequently increases the bond strength along with the increase in binding energy compared to that of K in K_2O [234]. The catalyst generated from other waste plant sources were also reported with similar binding energies of K [108,205,206]. The presence of two peaks at 346.49 and 350.20 eV in calcined catalyst, 346.95 and 350.47 eV in 3rd recycled catalyst and 346.40 eV in burnt ash catalyst (**Fig. 3.6** E) may be due to the existence of the oxide and carbonate of Ca in the catalysts [104,234]. The peaks at 102.05, 102.08 and 102.68 eV in the deconvoluted spectra of Si 2p (**Fig. 3.6** F) are exhibiting the binding energy of Si present in the form of SiO_2 found in the peduncle catalysts [206,234]. The elemental EDX {**Fig. 3.5** (D, E, F)} and XPS **(Fig. 3.6)** analyses of the catalysts demonstrated the occurrence of the leading composition of K in the form of K_2O and K_2CO_3 in the calcined catalyst which is expected to have major contributions to the catalysis of this study.

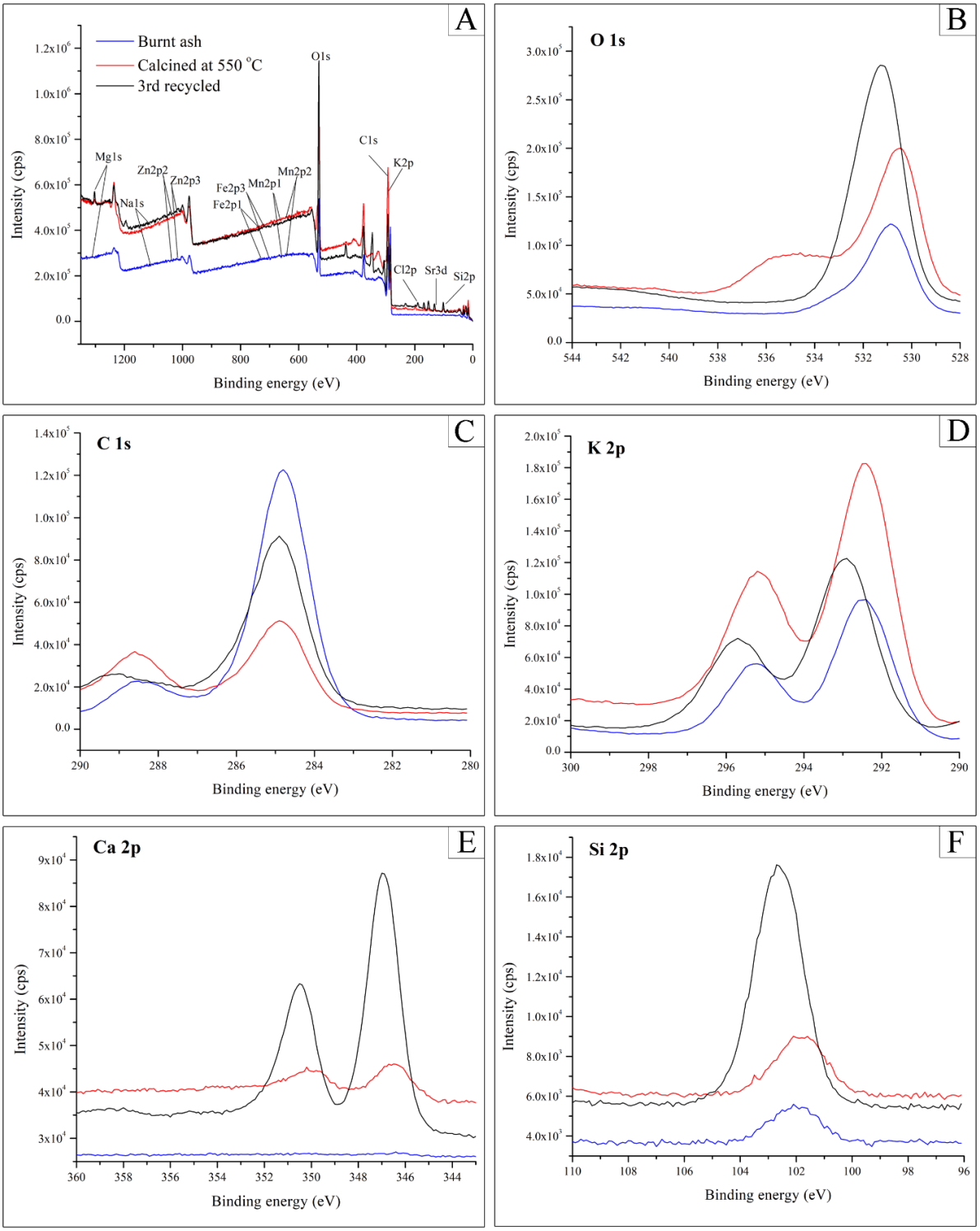

Fig. 3.6. (A) XPS survey spectra and XPS spectra of O 1s (B), C 1s (C), K 2p (D), Ca 2p (E) and Si 2p (F) of *M. champa* peduncle catalysts.

Table 3.3: XPS analysis of *Musa champa* peduncle catalyst

Elements	**Composition of *Musa champa* peduncle catalyst (Atomic %)**		
	Burnt ash	**Calcined at 550 °C**	**3rd recycled of 550 °C calcined**
C 1s	63.97	50.63	34.14
O 1s	22.56	23.01	32.11
K 2p	6.80	18.78	7.05
Ca 2p	0.04	0.05	3.52
Si 2p	4.83	5.71	19.33
Sr 3d	0.45	0.50	1.68
Mn 2p	0.27	0.18	0.25
Fe 2p	0.39	0.03	0.28
Zn 2p	0.32	0.29	0.24
Na 1s	0.15	0.05	0.09
Mg 1s	0.04	0.17	1.26
Cl 2p	0.18	0.66	0.04

3.3.1.6 HRTEM analysis

The structural information of the *M. champa* peduncle catalyst calcined at 550 °C is analyzed from HR-TEM images (**Fig. 3.7**), which exhibited the porous crystalline structure with an irregular shape. The TEM image (**Fig. 3.7** C) showed fringes of the materials indicating the porous characteristics of the catalyst. The porous character of the catalyst was also demonstrated in BET and BJH studies (**Fig. 3.4**). The Gatan microscopic analysis of the TEM image (**Fig. 3.7** C) revealed an interplanar distance (d value) of 0.3385 nm. The SAED pattern (**Fig. 3.7 D**) exhibited that the calcined catalyst was polycrystalline which is in agreement with the XRD analysis (**Fig. 3.2**) that demonstrated the presence of a mixture of crystalline components in the catalyst. The polycrystalline material was also described in the plant-based catalyst prepared from *Eichhornia crassipes* [135].

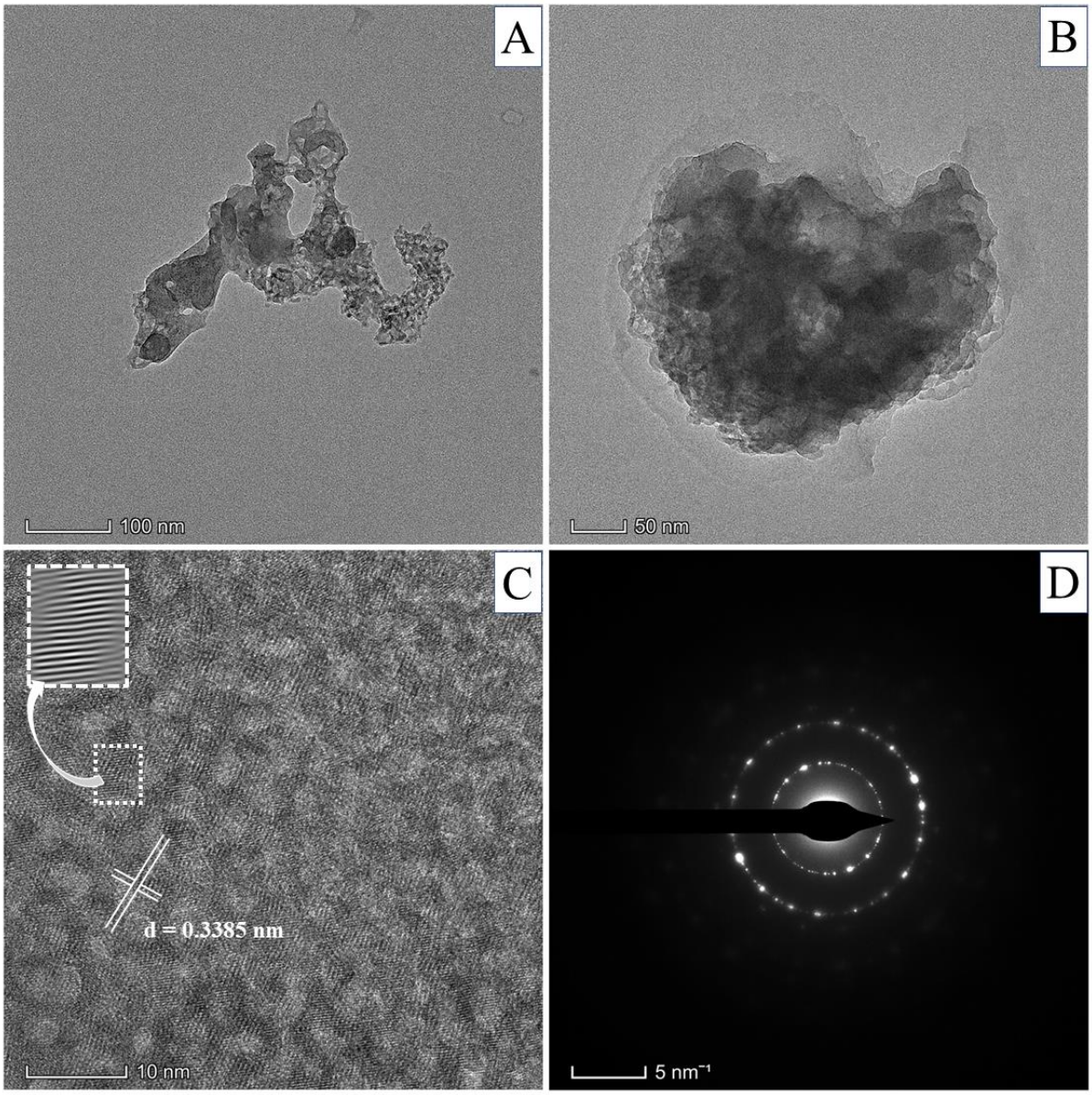

Fig. 3.7. HRTEM images (A, B, C) of *M. champa* peduncle catalyst calcined at 550 ^{o}C and its SAED pattern (D).

3.3.1.7 Measurement of pH value

The pH values of *M. champa* peduncle catalysts were measured and depicted in **Fig. 3.8**. The catalyst calcined at 550 ^{o}C displayed a pH value of 13.4 at 1:5 (w/v) and gradually decreased to 12.0 at 1:30 (w/v) indicating highly basic character. The burnt ash catalyst showed lower pH values in comparison to the calcined catalyst at the corresponding ratios. The higher pH value of the calcined catalyst may be credited due to the higher K content which was exposed from EDX (**Table 3.1**) and XPS (**Table 3.3**) analyses. The pH value of 13.5 for *M. paradisiaca* trunk catalyst [169] was also reported, and the catalyst was applied in biodiesel synthesis.

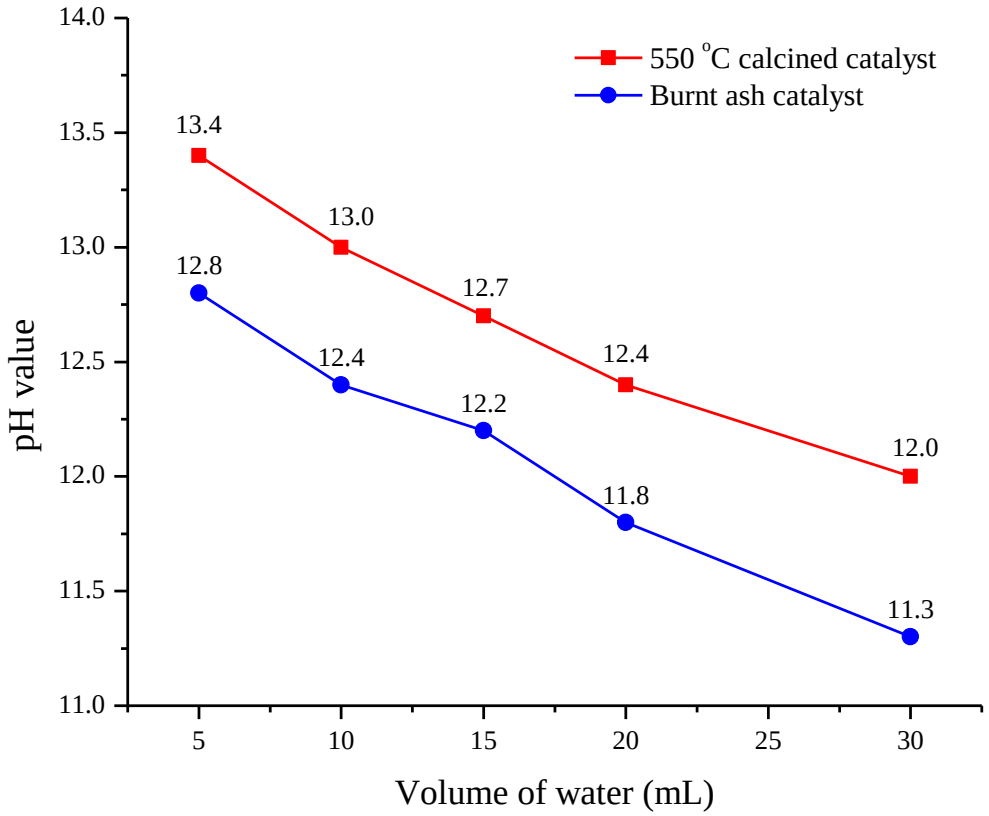

Fig. 3.8. Variation of pH value of *M. champa* peduncle catalysts (1 g) with different volume of water.

3.3.1.8 Determination of soluble alkalinity

The values of soluble alkalinity of *M. champa* peduncle burnt ash and calcined catalyst in water were 3.98 and 4.62 mmol g^{-1}. Comparable soluble alkalinity of 3.7 mmol g^{-1} was reported by Mendonça et al. [12] for tucumã peel catalyst that was calcined at 800 ºC and utilized for biodiesel synthesis. The catalysts from *M. paradisiaca* peel, trunk and rhizome also exhibited comparable soluble alkalinity values of 4.03, 5.10 and 5.43 mmol g^{-1} [169]. Noticeably greater soluble alkalinity value of 12.7 mmol g^{-1} was reported by Sharma et al. [136] for activated wood ash calcined at 800 ºC. However, a comparatively lower alkalinity value of 1.05 mmol g^{-1} for cupuaçu catalyst calcined at 800 ºC was reported by Mendonça et al. [44] and employed the catalyst in biodiesel production. The soluble alkalinity found in the *M. champa* catalyst demonstrated higher concentrations of metal carbonates and/or phosphates in the catalyst [44,136,169]. The XRD (**Fig. 3.2**), FTIR (**Fig. 3.3**) and XPS (**Fig. 3.6**) studies supported the presence of K_2CO_3 and K being the dominant element among the metals (**Table 3.1, Table 3.3**). In this study, the soluble alkalinity of the calcined catalyst was estimated in methanol also as the methanol was used in the transesterification and the value was found to be 1.06 mmol g^{-}

^{1}. This value is lower compared to that found in water (4.62 mmol g^{-1}) and this may be due to the lower polarity of methanol than water indicating the low solubility of the catalyst in methanol [169].

3.3.1.9 Determination of basicity of the catalyst

The basic strength of *M. champa* peduncle burnt ash and the calcined catalyst was tested using the Hammett titration method [169]. The assessment of both the catalysts showed a color change with bromothymol blue (H_ = 7.2), phenolphthalein (H_ = 9.3) and Nile blue (H_ = 10.1). The catalysts did not show any color change with the indicator 4-nitroaniline (H_ = 18.4) and aniline (H_ = 27.0) during analysis. Therefore, the basic strength of *M. champa catalysts* falls in the range of 10.1 < H_ < 18.4. The *M. champa* peduncle calcined catalyst (550 ^{o}C, 2 h) with higher K content was found to be more basic with a basicity of 1.65 mmol g^{-1} compared to the burnt ash catalyst having basicity of 1.46 mmol g^{-1}. This basicity trend is in good agreement with pH analysis of the catalysts (**Fig. 3.8**) and EDX and XPS data (**Table 3.1, Table 3.3**). Comparable basicity values of 1.59, 1.43 and 1.39 mmol g^{-1} were reported for the heterogeneous catalysts generated from *M. paradisiaca* banana trunk, peel and rhizome, respectively and the catalyst displayed excellent efficacy in biodiesel production [169]. Lower basicity of 0.170 mmol g^{-1} for *Citrus sinensis* ash coated magnetic catalyst [254] and 0.0891 mmol g^{-1} for sugarcane bagasse catalyst [104] were reported which were also applied in biodiesel syntheses.

3.3.1.10 Determination of turnover frequency (TOF)

The TOF of peduncle burnt ash and calcined catalyst were determined based on the amount of the FAME obtained [104,169,234] and found to be 0.152 min^{-1} and 0.298 min^{-1}, respectively. The TOF value confirmed the higher efficiency of *M. champa* calcined catalyst over burnt catalyst in biodiesel synthesis. A lower TOF 0.109 min^{-1} (6.59 h^{-1}) for sugarcane bagasse catalyst with lower catalytic activity [104] was reported compared to the present *M. champa* calcined catalyst which displayed excellent efficacy in transesterification catalysis. However, a higher TOF of 0.62 min^{-1} to 2.47 min^{-1} for the modified rice-husk silica-functionalized with amine catalyst was reported in biodiesel synthesis [255]. In biodiesel synthesis of castor oil, Roy et al. [256] applied K-promoted lanthanum oxide catalyst with a lower TOF of 0.072 min^{-1}. TOF values of 68.24, 56.85 and 46.16 min^{-1} for the catalysts from trunk, peel and rhizome of *M. paradisiaca* were reported with comparable activities in transesterification reaction [169] to that of *M. champa* calcined catalyst of this study.

3.3.2 Catalytic activity of the *Musa champa* peduncle catalyst in biodiesel synthesis

3.3.2.1 Effect of catalyst loading

The catalyst plays a vital role in the reaction rate as well as the yield of product in biodiesel synthesis. The present study investigated the jatropha oil reaction to biodiesel using the calcined catalyst derived from *M. champa* peduncle by varying the amount of catalyst (3, 5, 7 and 9 wt. % of oil) with 12:1 MTOR at 65 ^{o}C and the results are shown in **Fig. 3.9**. This study disclosed that on increasing the loading of catalyst from 3 to 7 wt. %, the biodiesel yield increased noticeably from 91.22 to 98.23 % with a decrease of reaction time significantly from 20 min to 6 min, respectively. Further increase of the catalyst loading to 9 wt. % exhibited no significant increase in the product yield and no noteworthy improvement in reaction time (**Fig. 3.9**). These results are consistent with the reported data of *M. balbisiana* peel catalyst [109]. It can be stated that catalyst loading beyond the optimum level has no revert effect in biodiesel synthesis. In this study, with a high product yield of 98.23 % within a very short time of 6 min, the catalyst load of 7 wt. % was considered the optimum level for the reaction at 65 ^{o}C and MTOR of 12:1.

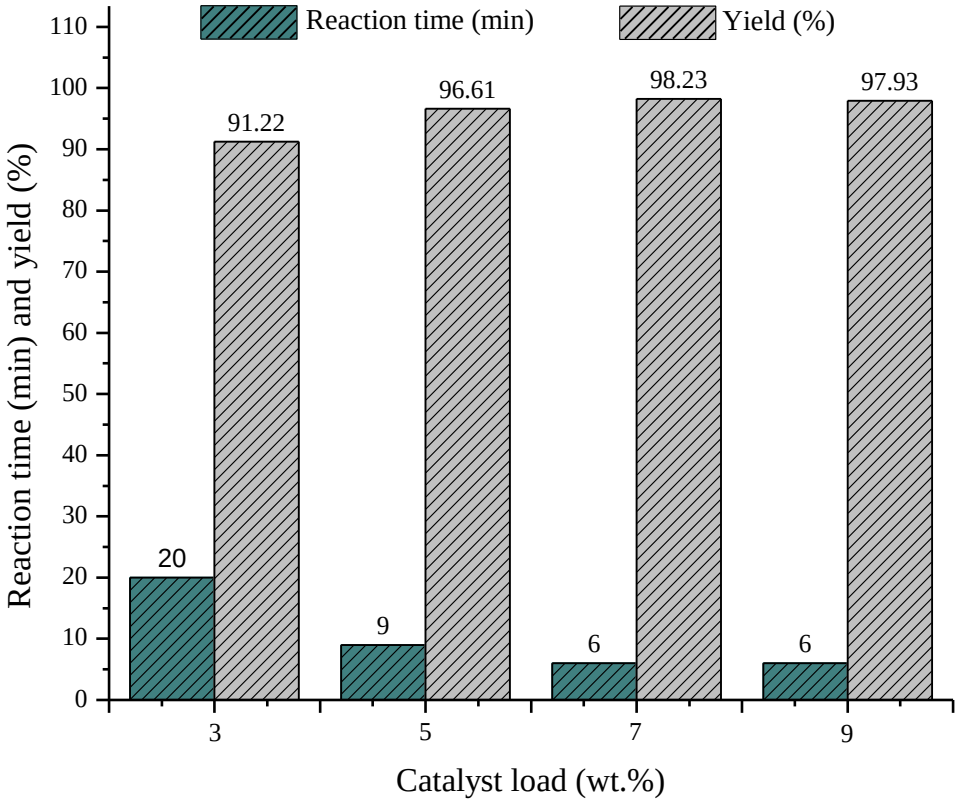

Fig. 3.9. Effect of peduncle calcined catalyst load on biodiesel production (MTOR = 12:1, Temperature = 65 ^{o}C).

3.3.2.2 Effect of methanol to oil ratio (MTOR)

The conversion of oil to biodiesel is believed to follow the kinetics of pseudo-first-order reaction and accordingly, an excess amount of methanol is needed for reaction completion [211,212,257]. However, reversible nature of the transesterification reaction and presence of large excess of methanol may revert the equilibrium towards the left, resulting in a decrease in product yield and complications of reaction completion. Thus, it is important to determine the optimum MTOR for the reaction and the reaction was carried out with the optimum catalyst load of 7 wt. % at 65 ^{o}C using different MTOR. This study (**Fig. 3.10**) demonstrated that on increasing the MTOR from 3:1 to 12:1, the yield also increased from 92.38 to 98.23 % with a substantial decrease in time of reaction from 12 min to 6 min (**Fig. 3.10**). Further increase in MTOR to 15:1 and 18:1, no improvement in terms of biodiesel yield and reaction time was noticed, instead, there is a slight decline in biodiesel yield (**Fig. 3.10**). The reason of this may be due to the utilization of excess of methanol at which there will be less interaction of catalyst with reactant because of dilution resulting in the decrease of reaction rate and product yield. Thus, in this study, a 12:1 MTOR is considered the optimum level for the reaction at 65 ^{o}C and 7 wt. % of catalyst loading. Analogous experimental observations were also reported for waste plant-generated catalyst by Syazwani et al. [230]. While studying the activities of various heterogeneous catalysts in biodiesel syntheses, similar levels of MTOR were also reported by Wang et al. [223], Taslim et al. [231], Uprety et al. [171] and Sharma et al. [136].

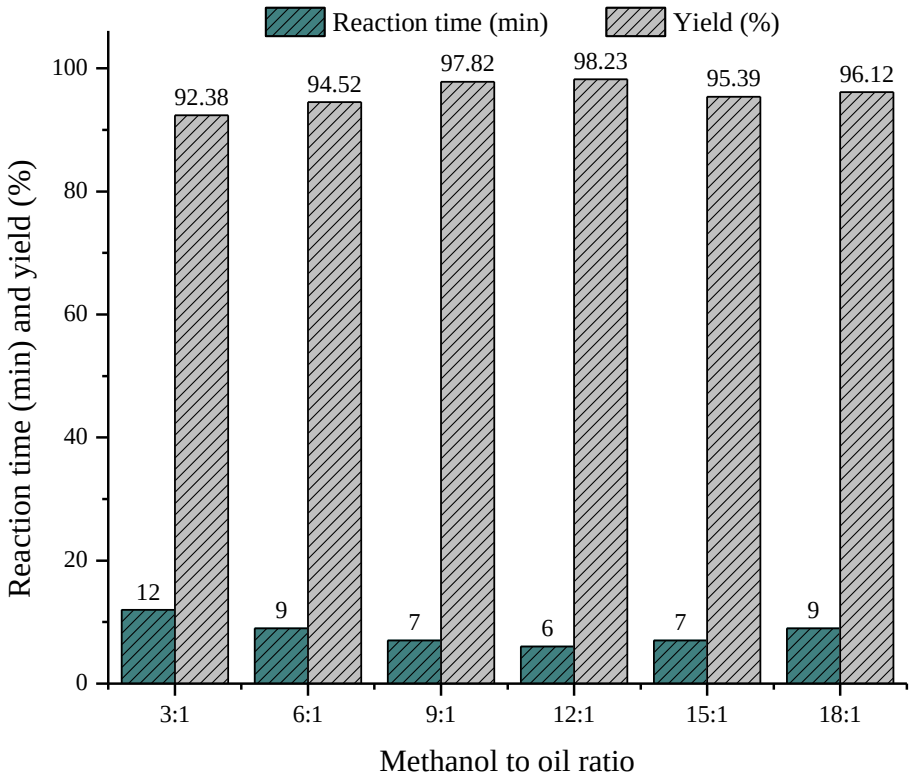

Fig. 3.10. Effect of MTOR on biodiesel production (Reaction temperature = 65 ^{o}C, calcined catalyst load = 7 wt.%).

3.3.2.3 Effect of temperature on the reaction

The influence of reaction temperature in the transesterification was investigated by changing temperatures at the ORCs of 7 wt. % of catalyst load and 12:1 MTOR. In this study, both *M. champa* peduncle calcined catalyst and burnt ash material were employed for the reaction and the results are depicted in **Fig. 3.11** and **Fig. 3.12**, respectively. The results demonstrated that when the temperature was raised from 25 to 65 ^{o}C, a noteworthy decline in reaction time from 70 to 6 min was noticed in the case of calcined catalyst and from 125 to 13 min in the case of burnt catalyst. At the same time, a substantial increase in biodiesel yield from 93.86 % (25 ^{o}C) to 98.23 % (65 ^{o}C) was observed with calcined catalyst and a similar trend was also seen in the case of burnt ash catalyst with the product yield from 86.76 % at 25 ^{o}C to 96.22 % at 65 ^{o}C. On the further increase of reaction temperature from 65 to 75 ^{o}C, there was no remarkable decrease in reaction time and no further improvement in biodiesel yield was noticed in both cases (**Fig. 3.11**, **Fig. 3.12**). In the study, more efficient performance of the reaction was found at 65 ^{o}C. Thus, 65 ^{o}C was considered the optimum temperature for both catalysts. Similarly, 65 ^{o}C was reported as the optimum temperature in several studies of biodiesel syntheses by Adesina et al. [232], Chouhan et al. [114], Odude et al. [106], Li et al.

[159], Basumatary et al. [169] and Sharma et al. [136]. From the results (**Fig. 3.11**, **Fig. 3.12**), it can be resolved that the calcined catalyst is better for the present study compared to the burnt ash material under the same reaction conditions and this can be well-supported by the catalyst characterization studies of EDX, XPS, pH value, basicity and TOF. Thus, the ORCs of the present study were 7 wt. % of catalyst amount, 12:1 MTOR and 65 ^{o}C of reaction temperature.

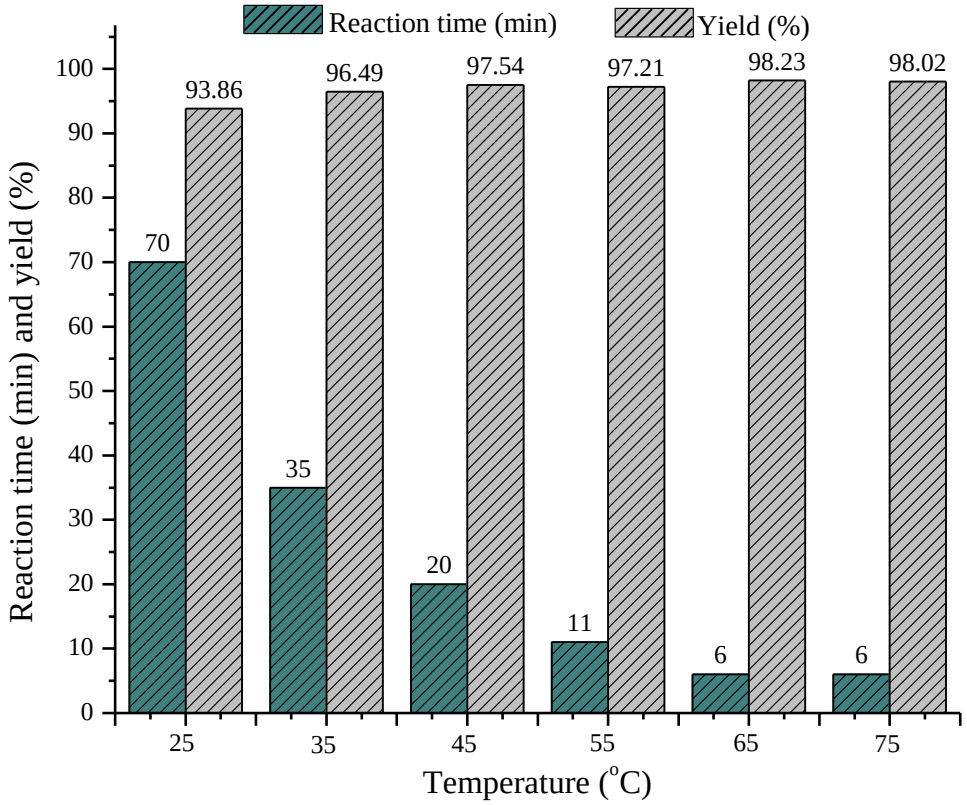

Fig. 3.11. Effect of reaction temperatures (25, 35, 45, 55, 65 and 75 ^{o}C) on biodiesel production using *M. champa* peduncle catalyst calcined at 550 ^{o}C (MTOR = 12:1, catalyst load = 7 wt.%).

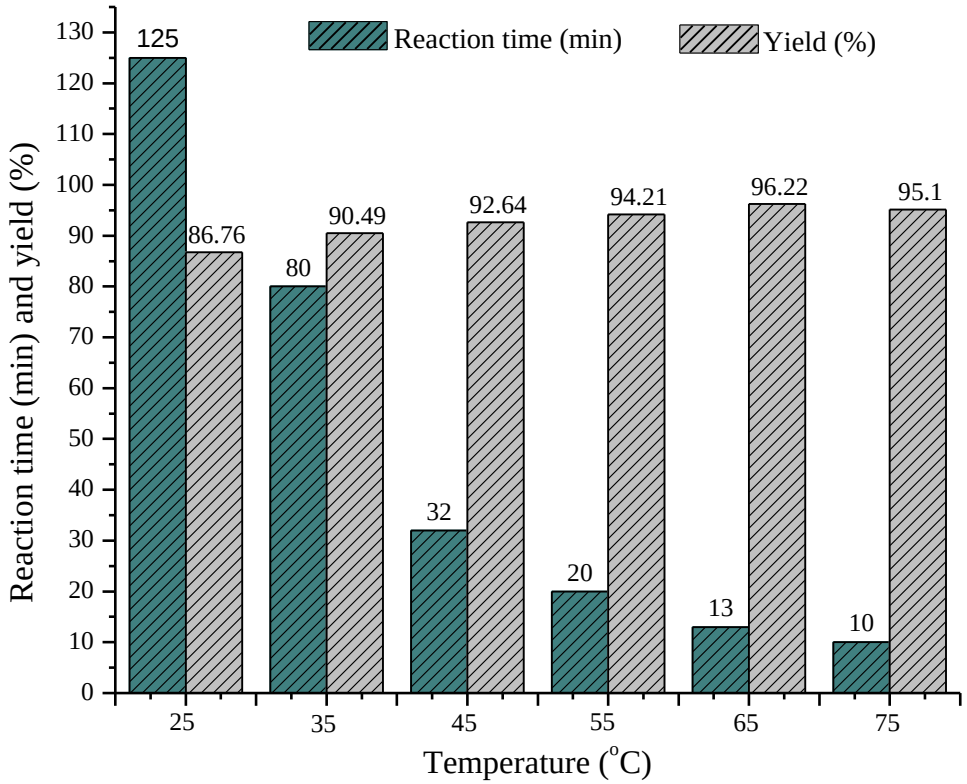

Fig. 3.12. Effect of reaction temperatures (25, 35, 45, 55, 65 and 75 ^{o}C) on biodiesel production using *M. champa* peduncle burnt ash catalyst (MTOR = 12:1, catalyst load = 7 wt.%).

3.3.3 Comparison of *M. champa* peduncle catalyst with other reported catalysts

The *M. champa* peduncle calcined catalyst under ORCs of 12:1 MTOR and 7 wt. % of catalyst at 65 ^{o}C could produce 98.23 % of jatropha biodiesel within the short reaction time of 6 min. At the same conditions, the burnt ash catalyst yielded 96.22 % of the product in 13 min. For comparison purposes, the results of solid catalysts prepared from other *Musa* species as well as other waste plant-based catalysts are listed in **Table 3.4**. **Table 3.4** discloses that catalysts generated from other *Musa* species showed a comparable yield of biodiesel. However, most of these catalysts were reported with a relatively longer reaction time than the present catalyst. Sarma et al. [111] and Aslam et al. [110] in their studies reported a very high reaction temperature of 275 ^{o}C and a longer reaction time (60 min) to achieve high biodiesel yield. This might be because of the lower basic character of their catalyst due to lower K content compared to the catalyst of this study.

Table 3.4: Activity comparison of *Musa champa* peduncle derived base catalyst in biodiesel synthesis with other reported agro-wastes ash catalysts

Biodiesel feedstock	**Catalyst source (Ash)**	**Calcination temp (°C)**	**Surface area ($m^2 g^{-1}$)**	**Parameter**				**Biodiesel, Y or C (%)**	**References**
				MTOR	**Catalyst (wt.%)**	**Temp (°C)**	**Time (min)**		
Jatropha oil	*Musa champa peduncle*	550	8.57	12:1	7	65	6	98.23 (Y)	This work
Jatropha oil	*Musa champa peduncle*	-	-	12:1	7	65	13	96.22 (Y)	This work
Jatropha oil	MBUS	550	38.71	9:1	5	275	60	98 (Y)	[111]
Mesua ferrea oil	MBUS	-	38.71	9:1	5	275	60	95 (C)	[110]
Jatropha oil	Malbhog peel	550	4.1	9:1	5	65	12	97.56 (Y)	[169]
Jatropha oil	Malbhog trunk	550	6.4	9:1	5	65	9	97.65 (Y)	[169]
Jatropha oil	Malbhog rhizome	550	7.0	9:1	5	65	14	95.67 (Y)	[169]
Thevetia peruviana oil	*Musa balbisiana* trunk	-	1.487	20:1	20	32	180	96 (Y)	[11]
Waste cooking oil	*Musa balbisiana* peel	700	10.176	6:1	2	60	180	100 (C)	[109]
Palm oil	Banana peel	-	-	3:2.4	4	65	65	99.5 (Y)	[106]
Soybean oil	*Musa acuminata* peel	-	1.4546	6:1	0.7	32	240	98.95 (C)	[108]

Soybean oil	Tucumã peels	800	1.0	15:1	1	80	240	97.3 (C)	[12]
Rapeseed oil	Gasified straw slag	--	1.266	12:1	20	200	480	95 (C)	[223]
Jatropha oil	*Lemna perpusilla*		9.622	9:1	5	65	300	89.43 (Y)	[114]
Palm oil	Birch bark	800	–	12:1	3	60	180	69.7 (C)	[171]
Soybean oil	K_2CO_3-Camphor tree ash	-	–	14:1	5	65	210	92.27 (Y)	[159]
Jatropha oil	$CaCO_3$-Wood ash	800	14.0	12:1	5	65	180	91.7 (C)	[136]
Jatropha oil	K_2CO_3-Wood ash	800	12.0	12:1	5	65	180	99 (C)	[136]
Jatropha oil	SrO-MBUS	550	0.043	9:1	5	200	60	96 (Y)	[197]
Waste cooking oil	KOH-Corncob ash	-	–	12:1	4	60	180	96 (Y)	[231]

MTOR–methanol to oil ratio; wt–weight; min–minute; Temp–temperature; C–conversion; Y–yield; MBUS–*Musa balbisiana* underground stem.

Table 3.4 also shows that other waste plant-based catalysts were reported with longer reaction times with comparable biodiesel yield to that of the present *M. champa* peduncle catalyst. Considering the reported results of the reactions (**Table 3.4**) and reported compositions of different catalysts (**Table 3.2**), the present peduncle catalyst exhibited superior catalytic efficacies for biodiesel synthesis. The attribution of better catalytic activity of *M. champa* peduncle catalyst may be due to its highly basic character because of higher K content (51.93 %) in the form of K_2CO_3 and K_2O (**Fig. 3.2**). Thus, the *M. champa* peduncle calcined catalyst can be considered as the potential catalyst in biodiesel generation along with cost-effectiveness and environmental friendliness character.

3.3.4 Reusability study of *Musa champa* peduncle catalyst

The reusability of *M. champa* peduncle catalyst calcined at 550 ^oC (2 h) was tested in transesterification of jatropha oil under the ORCs of 12:1 MTOR, 7 wt. % of catalyst and 65 ^oC. The catalyst after reaction completion was recovered by filtration using a suction pump followed by washing with n-hexane (4–5 times) and acetone (2–3 times). After washing, the catalyst was allowed to dry in the oven at 100 ^oC for 4 h, then cooled and reused in the next reaction cycle. The same process was followed for each reaction cycle. The result is presented in **Fig. 3.13**, which discloses that the catalyst could be efficiently reused up to the 3rd reaction cycle (4th run) with a decrease of biodiesel yield gradually from 98.23 % to 90.03 % (3rd cycle). The 3rd recycled catalyst was investigated with FE-SEM, EDX and XPS techniques to know the stability of the catalyst. From the FE-SEM images of the calcined catalyst (**Fig. 3.5** B) and 3rd recycled catalyst (**Fig. 3.5** C), a complete change in the surface morphology of the 3rd recycled catalyst was observed depicting the non-uniform sizes and shapes of sheet-like and layered type structures. This change may be the reason for decreased catalytic activity. The FE-SEM-EDX analyses of the catalysts (**Table 3.1**) indicated a reduction in the concentration of K from 51.93 % (fresh catalyst) to 13.20 % (3rd reused catalyst) and a similar trend was also noticed in XPS analyses of catalysts **(Table 3.3**). This leaching of K in the catalyst is demonstrating the decreased efficacy in catalysis and also exhibits that the K in the form of K_2O and K_2CO_3 are playing a crucial role in the reaction. In addition to the leaching of K components, there might be some coverage of the active sites of the catalyst by glycerol or ester molecules that may retard the effective interaction between catalyst-reagent leading to a decrease in catalytic efficiency [234]. Similar trends of recycled catalytic activities were also

reported for other waste biomass-based catalysts by Pathak et al. [108], Gohain et al. [109] and Sarma et al. [111].

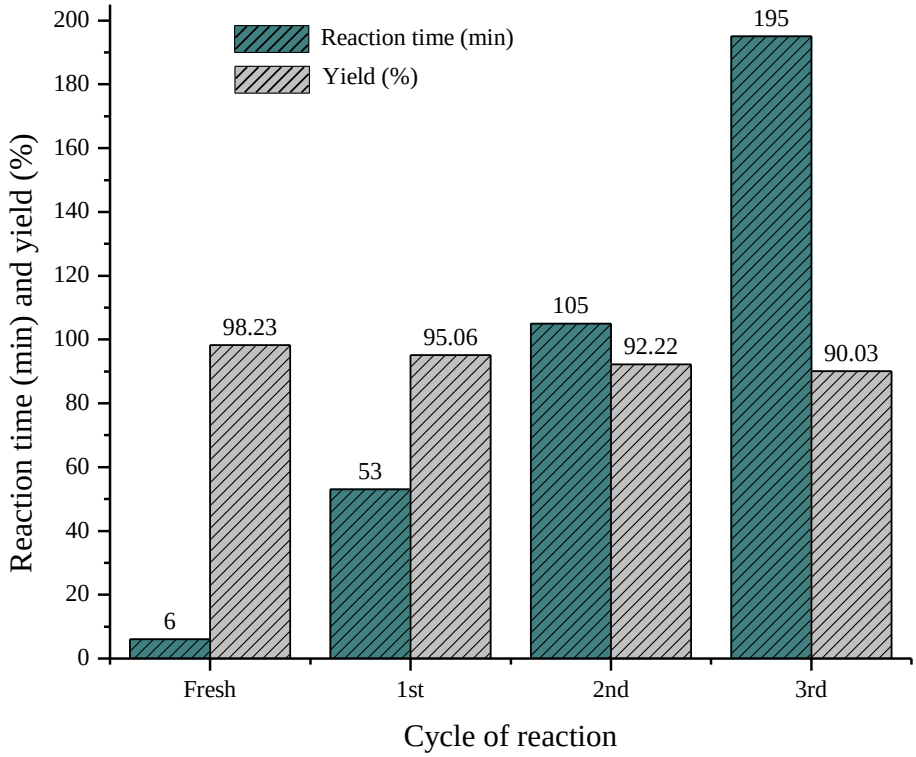

Fig. 3.13. Reusability study of *M. champa* peduncle catalyst calcined at 550 ^{o}C in jatropha biodiesel production (Reaction temperature = 65 ^{o}C, MTOR = 12:1, catalyst loading = 7 wt.%).

3.3.5 Kinetic and thermodynamic study

3.3.5.1 Determination of rate constant and order of reaction

The heterogeneous base-catalysed reaction of the oil with alcohol (mostly methanol) forming fatty acid esters (methyl esters) is believed to proceed through the three consecutive steps in which one mole of triglyceride (oil) reacts with three moles of CH_3OH yielding 3 moles of FAME as shown in the equations (3.1), (3.2), (3.3) and (3.4) [104].

$$\text{Triglyceride} + CH_3OH \rightleftharpoons \text{FAME} + \text{Diglyceride} \quad (3.1)$$

$$\text{Diglyceride} + CH_3OH \rightleftharpoons \text{FAME} + \text{Monoglyceride} \quad (3.2)$$

$$\text{Monoglyceride} + CH_3OH \rightleftharpoons \text{FAME} + \text{Glycerol} \quad (3.3)$$

$$\text{Triglyceride} + 3\,CH_3OH \rightleftharpoons 3\,\text{FAME} + \text{Glycerol} \quad (3.4)$$

To study the kinetics of jatropha oil transesterification using methanol and *M. champa* peduncle catalysts (calcined and burnt ash), the results obtained at various temperatures (25, 35, 45, 55, 65 and 75 ^{o}C) at the ORCs (MTOR = 12:1, catalyst load = 7 wt. %) were considered. The values obtained from the transesterification were put in the standard kinetic model equation of zero-order (3.5), first-order (3.6), pseudo-first order (3.7) and second-order (3.8) reactions and then the respective rate constants (k) were calculated [104].

$$\text{Zero-order reaction, } k = \frac{[TG]_o - [FAME]}{t} \quad (3.5)$$

$$\text{First-order reaction, } k = \frac{2.303}{t} \log \frac{[TG]_o}{[FAME]} \quad (3.6)$$

$$\text{Pseudo-first order reaction, } k = -\frac{2.303}{t} \log(1 - [FAME]) \quad (3.7)$$

$$\text{Second-order reaction, } k = \frac{1}{t} \times \frac{2.303}{([TG]_o - a)} \log \frac{a([TG]_o - x)}{[TG]_o(a - x)} \quad (3.8)$$

where, $[TG]_o$ = initial concentration of oil, [FAME] = concentration of produced FAME at time 't', a = initial concentration of CH_3OH (=12 as 12:1 MTOR is taken), x = $[TG]_o$ – [FAME] at time 't'.

The calculated rate constants are listed in **Table 3.5** (calcined catalyst) and **Table 3.6** (burnt ash catalyst). From the values of rate constant (k) so obtained, the Arrhenius plots are drawn and depicted in **Fig. 3.14–3.17** for the kinetic models of zero order, first order, pseudo-first-order and second-order reactions, respectively. The linear fitting of all the Arrhenius plots provided straight lines and the respective correlation coefficients (R^2 values) are listed in **Table 3.5** and **Table 3.6**. The Arrhenius best-fitted plot with the highest correlation coefficient is predicting the order of the reaction. Accordingly, biodiesel synthesis using the present *M. champa* peduncle calcined and burnt ash catalysts followed the pseudo-first order kinetics with the highest R^2 values of 0.96146 and 0.97063, respectively. Basumatary et al. [104,169] and Kaur et al. [212] also recently reported the pseudo-first-order kinetics for their studies of vegetable oil transesterification using methanol (excess) assisted by heterogeneous catalysts.

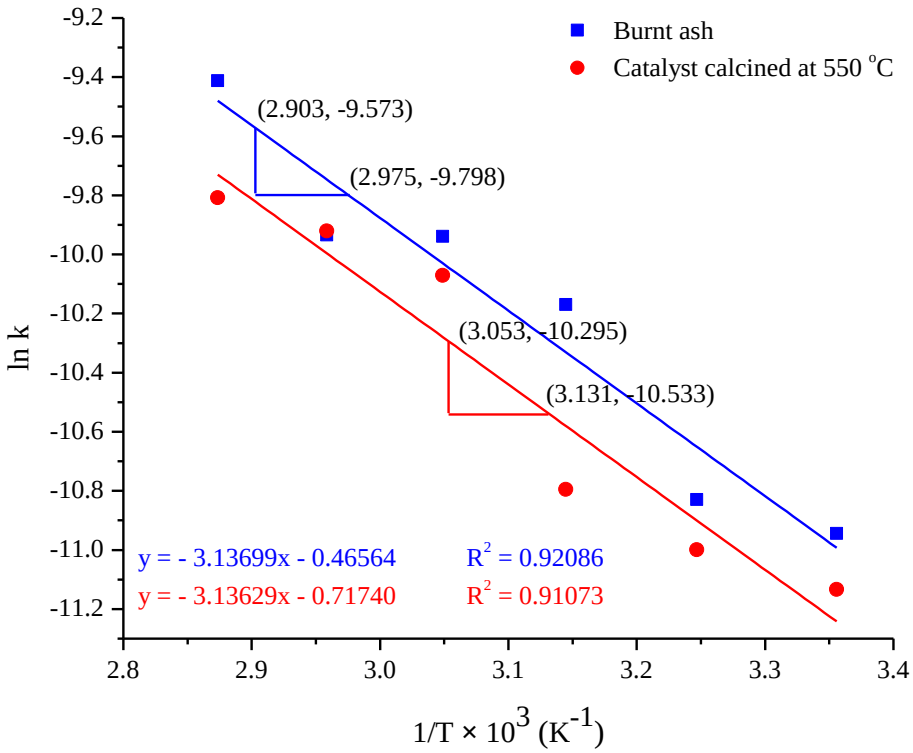

Fig. 3.14. Arrhenius plot (ln k versus $1/T\times10^3$) employing *M. champa* peduncle catalysts for the zero-order rate model (Reaction temperatures = 25, 35, 45, 55, 65 and 75 °C).

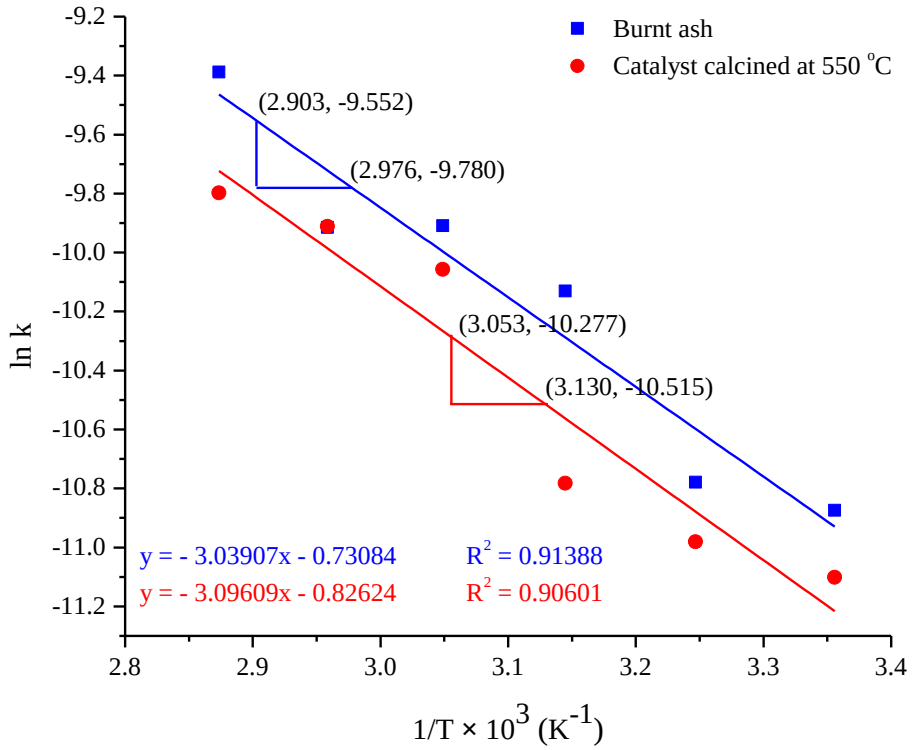

Fig. 3.15. Arrhenius plot (ln k versus $1/T\times10^3$) employing *M. champa* peduncle catalysts for the first order rate model (Reaction temperatures = 25, 35, 45, 55, 65 and 75 °C).

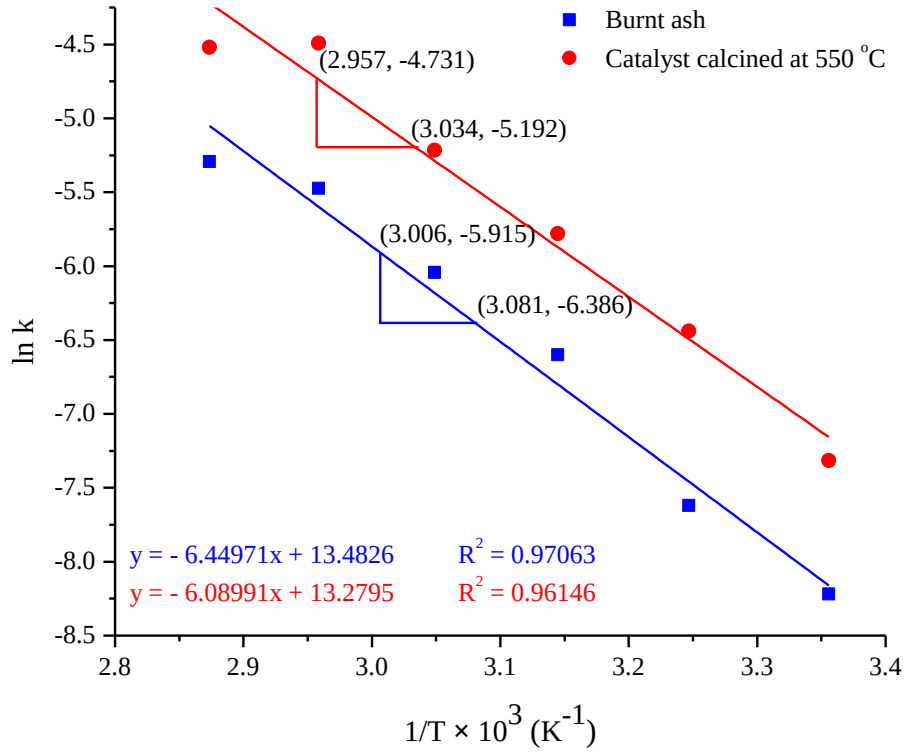

Fig. 3.16. Arrhenius plot (ln k versus $1/T\times10^3$) employing *M. champa* peduncle catalysts for the pseudo-first order rate model (Reaction temperatures = 25, 35, 45, 55, 65 and 75 °C).

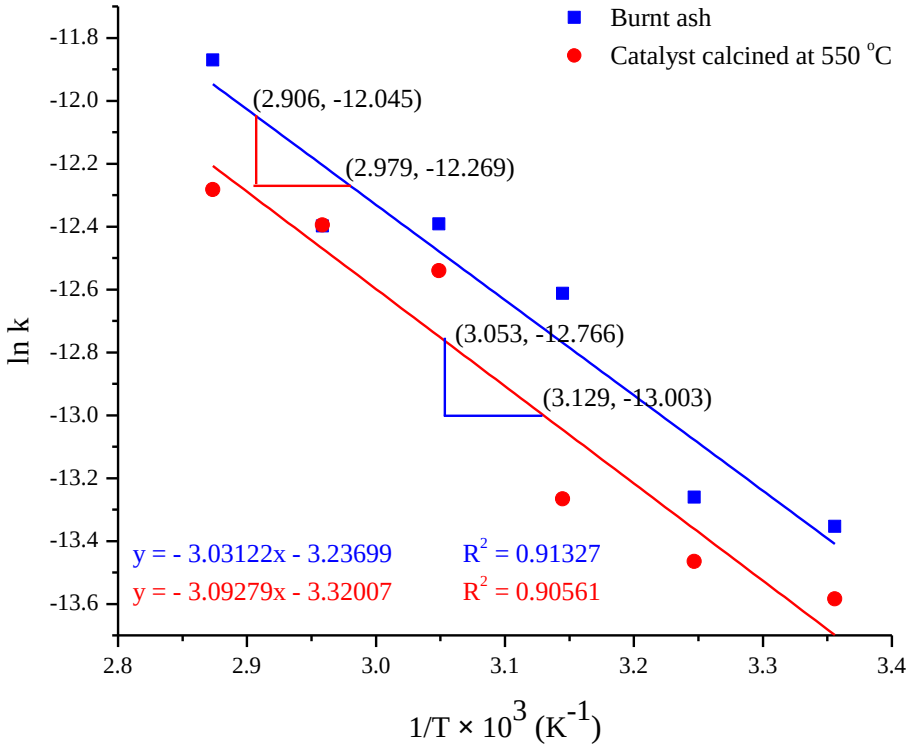

Fig. 3.17. Arrhenius plot (ln k versus $1/T\times10^3$) employing *M. champa* peduncle catalysts for the second order rate model (Reaction temperatures = 25, 35, 45, 55, 65 and 75 °C).

Table 3.5: Rate constant (k), correlation coefficient (R^2), activation energy (Ea) and pre-exponential factor (A) of various kinetic models for *Musa champa* peduncle burnt ash catalyst

Order of reaction	**Rate constant, k (s^{-1}) at various temperature (K)**						**R^2 value**	**Activation energy, Ea (kJ mol^{-1})**	**Pre-exponential factor, A (s^{-1})**
	298	**308**	**318**	**328**	**338**	**348**			
Zero order	1.77×10^{-5}	1.98×10^{-5}	3.83×10^{-5}	4.83×10^{-5}	4.85×10^{-5}	8.17×10^{-5}	0.92086	26.08	6.27×10^{-1}
First order	1.89×10^{-5}	2.08×10^{-5}	3.98×10^{-5}	4.97×10^{-5}	4.94×10^{-5}	8.38×10^{-5}	0.91388	25.27	4.81×10^{-1}
Pseudo-first order	2.69×10^{-4}	4.90×10^{-4}	1.35×10^{-3}	2.37×10^{-3}	4.19×10^{-3}	5.02×10^{-3}	0.97063	53.62	7.16×10^{5}
Second order	6.46×10^{-6}	7.06×10^{-6}	1.34×10^{-5}	1.67×10^{-5}	1.66×10^{-5}	2.81×10^{-5}	0.91139	26.08	1.47×10^{-1}

Table 3.6. Rate constant (k), correlation coefficient (R^2), activation energy (Ea) and pre-exponential factor (A) of various kinetic models for *Musa champa* peduncle catalyst calcined at 550 ^{o}C.

Order of reaction	**Rate constant, k (s^{-1}) at various temperature (K)**						**R^2 value**	**Activation energy, Ea (kJ mol^{-1})**	**Pre-exponential factor, A (s^{-1})**
	298	**308**	**318**	**328**	**338**	**348**			
Zero order	1.46×10^{-5}	1.67×10^{-5}	2.05×10^{-5}	4.23×10^{-5}	4.92×10^{-5}	5.50×10^{-5}	0.91073	26.08	4.89×10^{-1}
First order	1.51×10^{-5}	1.70×10^{-5}	2.08×10^{-5}	4.29×10^{-5}	4.96×10^{-5}	5.56×10^{-5}	0.90601	25.74	4.37×10^{-1}
Pseudo-first order	6.64×10^{-4}	1.59×10^{-3}	3.08×10^{-3}	5.42×10^{-3}	1.12×10^{-2}	1.09×10^{-2}	0.96146	50.63	5.85×10^{5}
Second order	5.08×10^{-6}	5.71×10^{-6}	6.95×10^{-6}	1.44×10^{-5}	1.66×10^{-5}	1.86×10^{-5}	0.90439	25.63	1.41×10^{-1}

3.3.5.2 Determination of activation energy (Ea) and pre-exponential factor (A)

The values of E_a and A were determined from the slopes (= E_a/R, R = 8.314 J K^{-1} $mol^{-}1$, the universal gas constant) and the intercepts (= ln A) of the respective straight lines of the Arrhenius plots (**Fig. 3.14–3.17**). The results are presented in **Table 3.6** (calcined catalyst) and **Table 3.5** (burnt ash catalyst). As per the obtained pseudo-first order kinetics (**Fig. 3.16**), the calculated activation energies of 50.63 and 53.62 kJ mol^{-1} and pre-exponential factors (frequency factors) of 5.58×10^5 and 7.16×10^5 s^{-1} were found for the calcined catalyst and burnt ash catalyst, respectively. The calculated values of activation energy for both the catalysts of this study were found within the range of 21–84 kJ mol^{-1} reported for the synthesis of biodiesel [205,212,257,258]. Mendonça et al. [12] reported a higher value of Ea of 61.23 kJ mol^{-1} for their biodiesel synthesis than the present study. Thus, the *M. champa* peduncle catalyst with a good Ea value is competent enough in catalyzing the reaction of jatropha oil to biodiesel.

3.3.5.3 Study of thermodynamic parameters

Following the Eyring-Polanyi equation (3.9) [104,259,260], the values of the thermodynamic parameters, change in entropy (ΔS) and change in enthalpy (ΔH) were determined from the slope (-ΔH/R) and intercept (ln (k_b/h) + ΔS/R) of the straight lines obtained by the linear fitting of the Eyring-Polanyi plots (ln k/T versus $1/T\times10^3$) (**Fig. 3.18**). The value of Gibbs free energy change (ΔG) for the transesterification was calculated from the equation (3.10) and the results are presented **Table 3.7**.

$$\ln\left(\frac{k}{T}\right) = -\left(\frac{\Delta H}{RT}\right) + \left[\ln\left(\frac{k_b}{h}\right) + \frac{\Delta S}{R}\right] \quad (3.9)$$

$$\Delta G = \Delta H - T\Delta S \quad (3.10)$$

where h = 6.626×10^{-34} J.s (Planck constant), k_b = 1.38×10^{-23} J K^{-1} (Boltzmann constant) and T = absolute temperature (K).

The values of ΔH were found to be +47.96 and +50.95 kJ mol^{-1} K^{-1} using the calcined catalyst and burnt ash catalyst, respectively. These resultant positive ΔH values are demonstrating the endothermic pathway and the reaction proceeds via an external supply of heat energy [234]. A positive ΔH value was also reported in the studies of Roy et al. [259], Basumatary et al. [104], Banerjee et al. [260] and Sarve et al. [261], which are indicative of the endothermic reaction (ΔH>0). In the present study, negative ΔS values were obtained (**Table**

3.7). The negative value of ΔS also asserted the utilization of supplied energy to the system as well as the endothermic mode of the reaction pathway [104]. The values of change in the Gibbs free energy (ΔG) for the transesterification using both the catalysts were calculated and positive ΔG values were found (**Table 3.7**). The positive value of ΔG (ΔG>0) is representing the non-spontaneous and endergonic reaction and the present study is in well-agreement with the results reported for the transesterification reactions using waste sugarcane catalyst [104] and mesoporous calcium titanate [257].

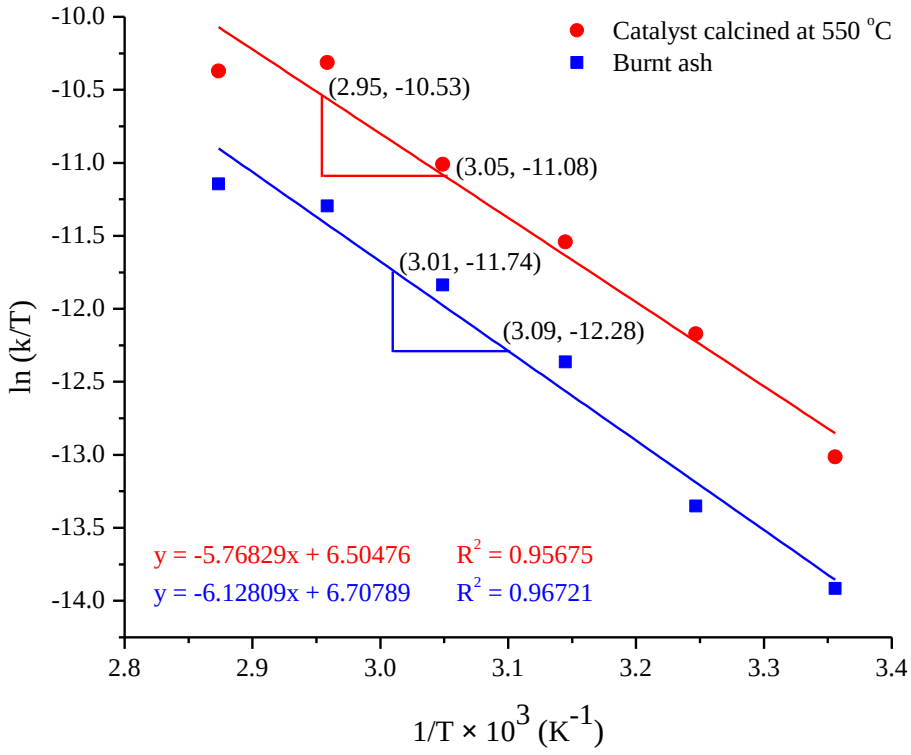

Fig. 3.18. Eyring-Polanyi plot (ln (k/T) versus 1/T×10^3) of *Musa champa* peduncle burnt ash and calcined at 550 °C catalyst.

Table 3.7: Thermodynamic parameters of the reaction catalysed by *Musa champa* peduncle burnt ash and calcined at 550 °C

Thermodynamic parameters/ Catalysts	**ΔH° (kJ mol^{-1} K^{-1})**	**ΔS° (kJ mol^{-1} K^{-1})**	**ΔG° (kJ mol^{-1})**					
			298 K	**308 K**	**318 K**	**328 K**	**338 K**	**348 K**
Burnt ash	50.95	-0.142	93.19	94.61	96.03	97.45	98.86	100.28
Calcined at 550 °C	47.96	-0.143	90.71	92.14	93.57	95.01	96.44	97.88

3.3.6 Characterization of *J. curcas* biodiesel

3.3.6.1 FT-IR analysis

The FT-IR patterns of the oil and biodiesel are presented in **Fig. 3.19**. The peak at 1746 cm^{-1} is due to the stretching vibration of C=O (carbonyl) group of the triglyceride and the peak at 1742 cm^{-1} in biodiesel is due to C=O stretching vibration of the methyl esters (RCOOMe) (**Fig. 3.19**). This change is indicative of the transformation of one ester (oil) to another ester (FAME). The peak at 3002 cm^{-1} is representing the stretching frequency of =C-H group (-CH=CH-) present in the fatty acid chain of both the oil and FAME. The C-H stretching vibrations in the oil and FAME are seen at 2852 and 2925 cm^{-1}. The peaks due to bending vibrations of the CH_3 groups present are noticed at 1465 and 1379 cm^{-1} in the oil and at 1461 and 1436 cm^{-1} in the FAME. The C-O stretching bands of jatropha oil are characterized by the peaks at 1239, 1162, 1113 and 1094 cm^{-1} and that of biodiesel is at 1249, 1362, 1199, 1172, 1120 and 1015 cm^{-1}. The signals at 723 cm^{-1} in the case of oil and FAME are depicting the rocking of the -CH_2- group of the fatty acid chain.

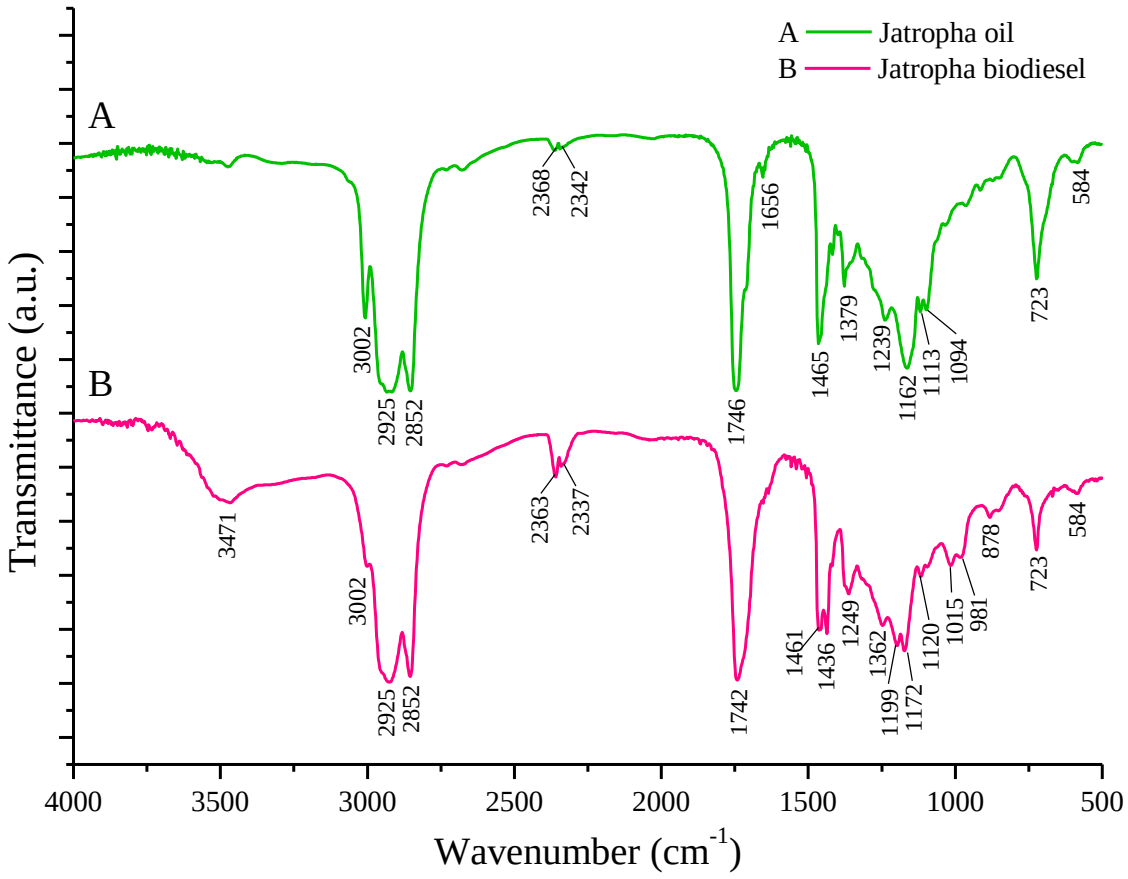

Fig. 3.19. FT-IR spectra of jatropha oil (A) and its biodiesel (B).

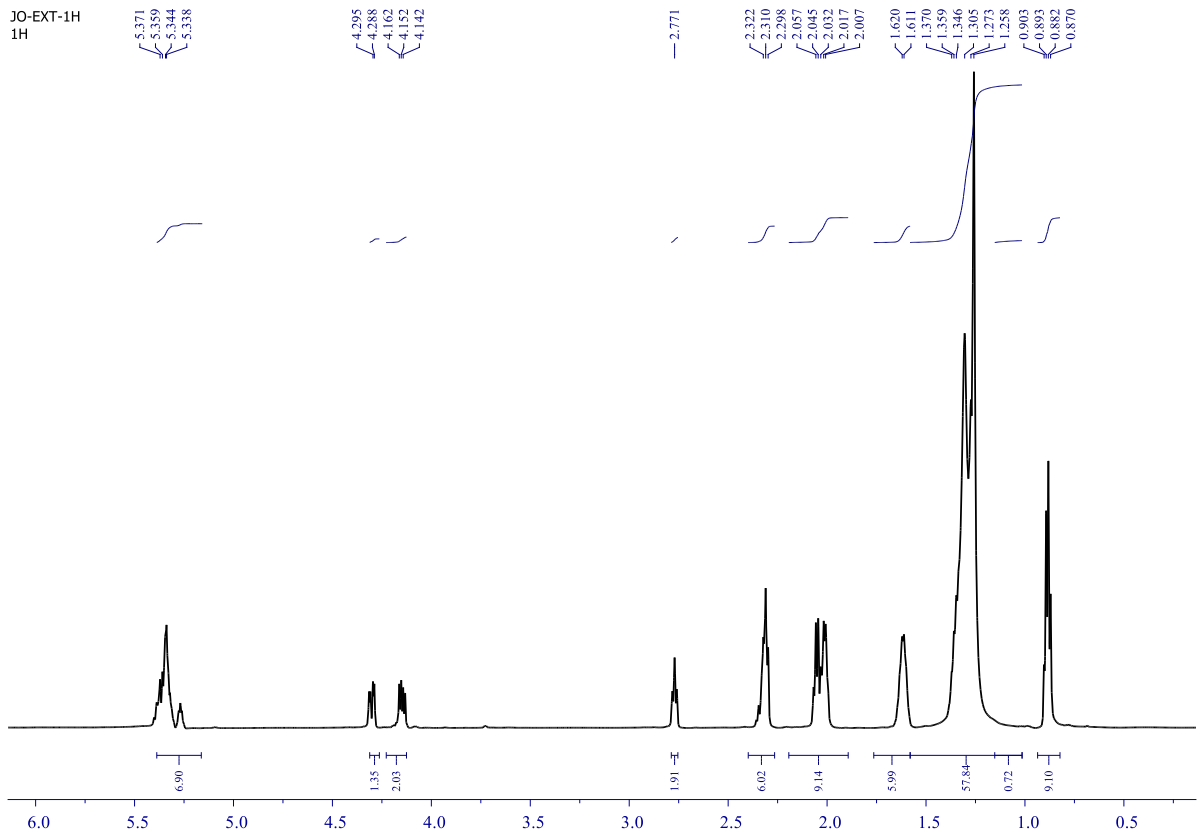

Fig. 3.20. 1H-NMR spectrum of jatropha oil.

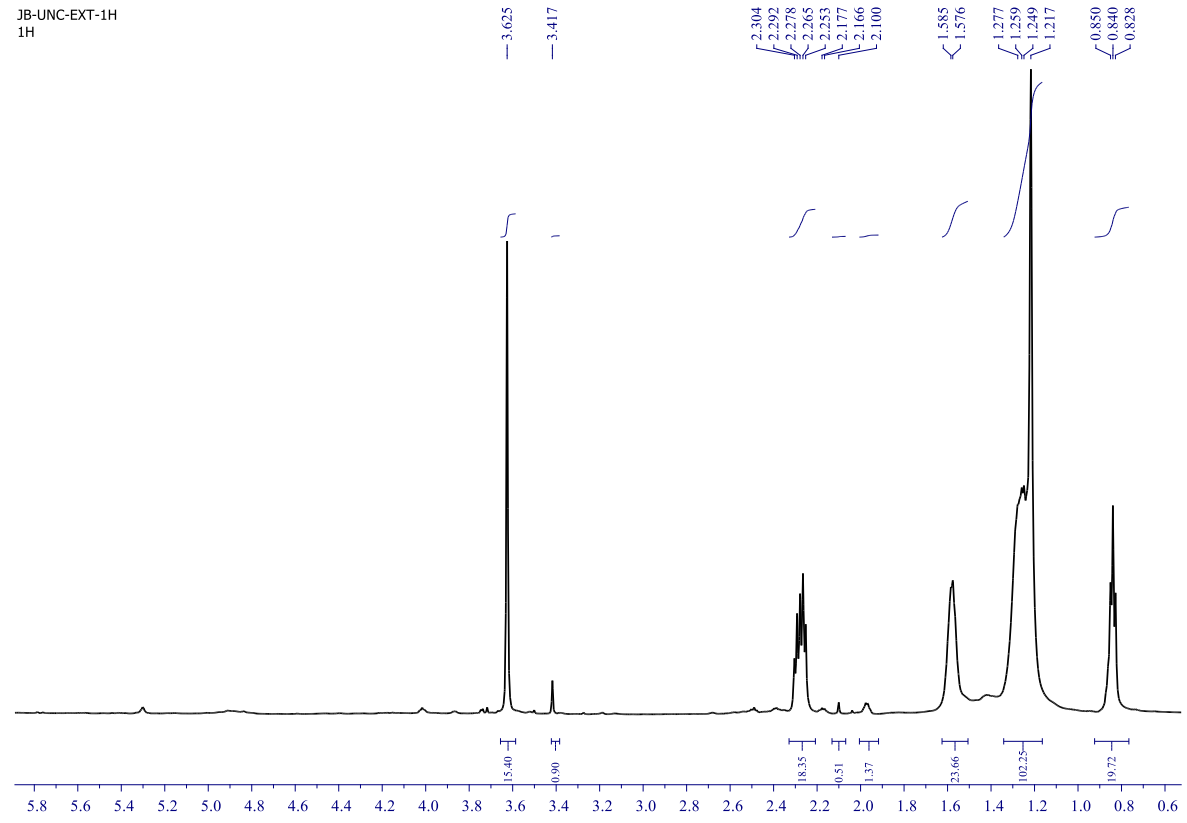

Fig. 3.21. ^{1}H-NMR spectrum of jatropha biodiesel.

3.3.6.2 FT-NMR analysis

The recorded ^{1}H-NMR spectra of the oil and FAME are shown in **Fig. 3.20** and **Fig. 3.21**, which showed the formation of FAME. The presence of methine (-C***H***-) proton at C2 of triglyceride (-C***H***-CO_2R) showed a signal at δ 5.338-5.344 ppm and methylene (-C***H***$_2$-) proton at C1 and C3 of triglyceride (-C***H***$_2$-CO_2R) displayed signals at δ 4.142-4.295 ppm (**Fig. 3.20**). These signals disappeared in the ^{1}H-NMR pattern of FAME (**Fig. 3.21**), where the appearance of a new singlet signal at δ 3.625 ppm was noticed due to the methoxy protons (-COOC***H***$_3$) of FAME. These changes confirmed the transformation of oil to FAME.

3.3.6.3 GC-MS analysis of *J. curcas* biodiesel

The composition of jatropha biodiesel studied with the GC-MS technique (**Fig. 3.22**) is listed in **Table 3.8**, which revealed the presence of six different types of saturated and unsaturated fatty acid esters. The methyl oleate, an unsaturated fatty acid ester, was found to be the predominant one with 39.236 % followed by methyl linoleate (30.45 %) and methyl palmitate with 20.45 % being the major saturated component. The saturated fatty acid esters such as methyl stearate and methyl arachidate with 5.61 and 1.305 % respectively were also found to be present.

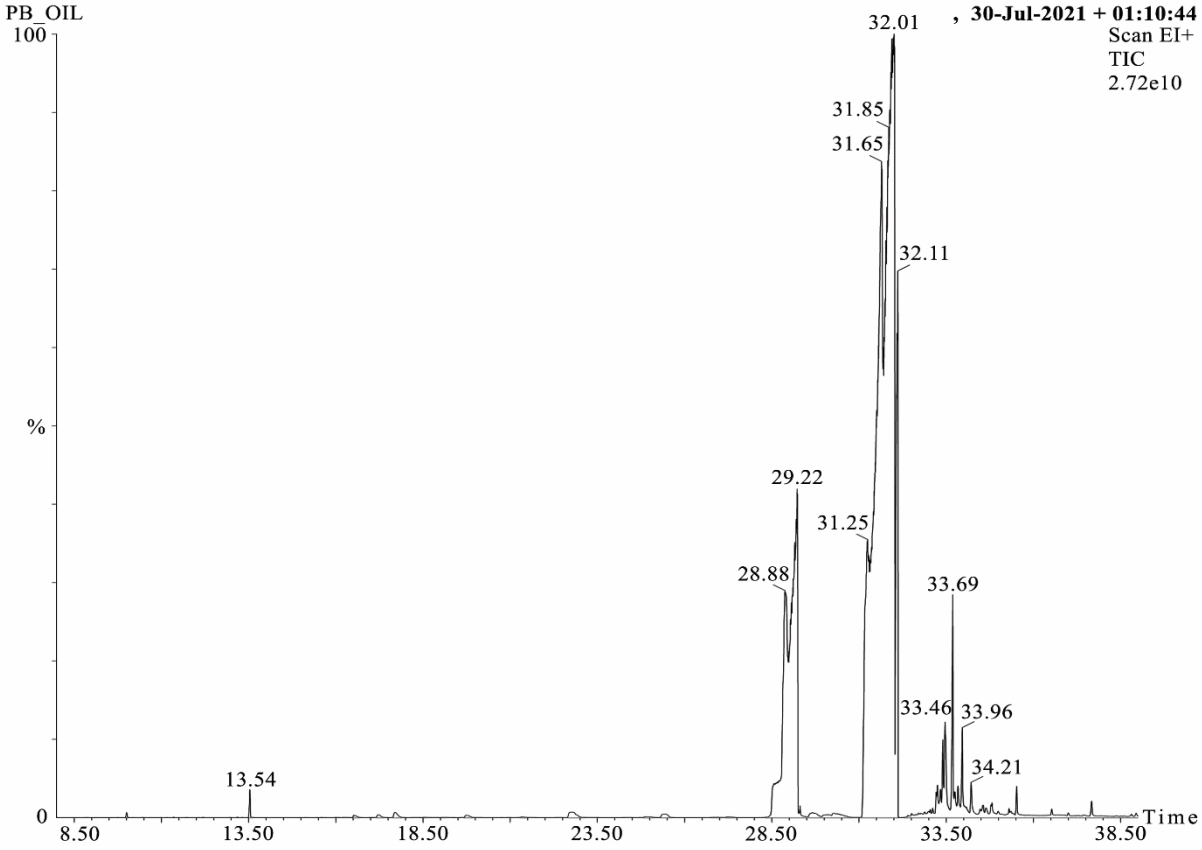

Fig. 3.22. GC spectra of jatropha biodiesel.

Table 3.8: GC-MS analysis of jatropha biodiesel

RT	Methyl ester (FAME) composition of biodiesel	Composition (%)
29.22	Methyl palmitate [C16:0]	20.450
31.65	Methyl linoleate [C18:2]	30.450
32.01	Methyl oleate [C18:1]	39.236
32.11	Methyl stearate [C18:0]	5.610
33.46	Methyl gondoate [C20:1]	0.949
33.69	Methyl arachidate [C20:0]	1.305

3.3.7 Fuel properties of the *J. curcas* biodiesel

The biodiesel properties of this study were investigated and compared with the standards and other reported biodiesels (**Table 3.9**). The density of jatropha biodiesel at 15^{o}C (0.8906 g cm^{-3}) was found within EN 14214 limit and comparable to the results of other reported biodiesels [109,114] (**Table 3.9**). The kinematic viscosity at 40 ^{o}C was 5.580 mm^2 s^{-1} and was found to be in the range of standard ASTM D6751. This value is comparable to the data reported by Sarma et al. [111] and lower compared to the value reported by Chouhan and Sarma [114]. The cetane number of 49.4 for the biodiesel was obtained which is above the specified minimum value of ASTM D6751. This value is higher compared to the data reported by Sarma et al. [111], Odude et al. [106] and Kumar et al. [197]. Higher cetane numbers were reported in the works of Basumatary et al. [208,234], Adesina et al. [232] and Deka and Basumatary [11] (**Table 3.9**). In the present study, the cetane index was recorded as 55.58. The pour point (^{o}C) and cold filter plugging point (^{o}C) were found to be 0 and <4, respectively. The acid value of biodiesel was found to be 0.364 mg of KOH/g which is quite below the maximum limit specified in the standards (**Table 3.9**). The saponification value of the produced biodiesel was calculated as 189.06 mg KOH/g which is close to the reported data [205,206,208,234]. The degree of unsaturation (iodine value) calculated was found to be 87.03 g I_2/100 g which satisfied the EN 14214 standard. The American petroleum index, diesel index and aniline index were determined as 34.278, 70.043 and 204.342, respectively. The HHV (Higher heating value) of 41.226 MJ kg^{-1} was achieved for the jatropha biodiesel of this study and found to be well-comparable with the reported data (**Table 3.9**).

Table 3.9: Comparison of fuel properties of the produced biodiesel with ASTM D6751, EN 14214 and reported properties

Properties	**ASTM D6751**	**EN 14214**	**Jatropha biodiesel (This study)**	**Reported biodiesel**								
				Jatropha oil [114]	**Jatropha oil** [111]	**Jatropha oil** [197]	**Palm oil** [232]	**Yellow oleander oil** [11]	**Palm oil** [106]	***Gmelina arborea* oil** [208]	**WCO** [109]	**WCO** [220]
Density (15 ^{o}C, g/cm^{3})	NS	0.86-0.90	0.8906	0.891	0.875	0.875	-	0.875	-	0.877	0.89	0.87
Kinematic viscosity (40 ^{o}C, mm^{2}/s)	1.9-6.0	3.5-5.0	5.580	6.8	5.7	4.75	4.3	4.33	4.7	-	3.12	3.10
Cetane number	47 (min)	51 (min)	49.4	-	48.6	48.3	76.93	61.5	44.4	64.2		-
Cetane index	NS	NS	55.58		-		-	62.9	-	-	55	57
Acid value (mg of KOH/g)	0.50 (max)	0.50 (max)	0.364	0.0	4.0	4.6	0.4	0.057	0.5	0.105	0.08	0.06
Pour point (^{o}C)	NS	NS	0	-	3	-6	-6	3	-3	-	-9	-10
CFPP (^{o}C)	NS	NS	<4	-	-	-	-	6	-	-	-	-

Saponification number (mg KOH/g)	NS	NS	189.06	-	-	-	-	-	-	185.7	-	-
Iodine value (g I_2/100 g)	NS	120 (max)	87.03	-	119	74.5	40.90	69.9	24.7	51.0	-	-
API	36.95	NS	34.278	0.892	0.875	-	32.42	-	30.51	-	-	-
Diesel index	50.4	NS	70.043	-	-	-	92.95	-	47.87	-	-	-
Aniline index	331	NS	204.342	-	-	-	-	-	-	-	-	-
HHV (MJ/kg)	NS	NS	41.226	37.1	39.25	38.35	-	44.986	-	40.7	40.20	40.30

Min–minimum; max–maximum; NS–not specified; CFPP–cold filter plugging point; API–American petroleum index; HHV–higher heating value (calorific value); WCO–Waste cooking oil.

3.4 Conclusion

A highly efficient heterogeneous catalyst could be developed in this study from the waste *M. champa* peduncle and successfully utilized in biodiesel preparation from *J. curcas* oil. The XRD analysis exposed the occurrence of metal carbonates and oxides in the catalysts. The calcined catalyst (550 ^{o}C, 2 h) due to the existence of a higher amount of K (51.93 wt. % in EDX, 18.78 atomic % in XPS) in the form of oxide and carbonate exhibited superior efficacy in catalysis than the burnt ash catalyst which has lower K concentration. An excellent biodiesel yield of 98.23 % was found under ORCs of 12:1 MTOR and 7 wt. % of calcined catalyst at 65 ^{o}C in short reaction time of 6 min. The calcined catalyst exhibited a micro-mesoporous structure with a surface area of 8.57 m^2 g^{-1} and showed higher basicity of 1.65 mmol g^{-1} with TOF of 0.298 min^{-1} compared to that of the burnt ash catalyst. The reusability study showed a high yield of 90.03 % biodiesel in the 3rd reaction cycle. Kinetic studies demonstrated the pseudo-first-order reaction with Ea values of 50.63 and 53.62 kJ mol^{-1} and A (pre-exponential factor) values of 5.58×10^5 and 7.16×10^5 s^{-1} for the calcined catalyst and burnt ash catalyst, respectively. The endothermic pathway ($\Delta H>0$) and non-spontaneous ($\Delta G>0$) and endergonic nature of the reaction could be revealed from the thermodynamic studies. Thus, the environmental benign *M. champa* peduncle heterogeneous catalyst is being developed from easily available and low-cost natural post-harvest materials. This catalyst could play a noteworthy role in the cost-effective synthesis of biodiesel as well as may find a suitable place for the biorefinery scale application.